



PERGAMON

Deep-Sea Research I 49 (2002) 1623–1649

DEEP-SEA RESEARCH
PART I

www.elsevier.com/locate/dsr

Sea ice biological communities and nutrient dynamics in the Canada Basin of the Arctic Ocean

Igor A. Melnikov^{a,*}, Elena G. Kolosova^b, Harold E. Welch^c, Ludmila S. Zhitina^b

^a *P.P. Shirshov Institute of Oceanology, 117851 Moscow, Russia*

^b *M.V. Lomonosov Moscow State University, 117234 Moscow, Russia*

^c *Fresh Water Institute, Winnipeg, Canada*

Received 16 January 2002; accepted 20 May 2002

Abstract

Salinity, concentrations of silicate (Si), phosphate (P), and chlorophyll *a* (chl *a*), and the species composition of floral and faunal communities were assessed in multi-year (MY) and first-year (FY) ice, and at the water–ice interface, during the SHEBA ice camp drift in the Canadian Basin of the Arctic Ocean, October 1997–October 1998. Mean integrated salinity values varied from $0.1 \pm 0.8\text{‰}$ within the snow–ice boundary to $3.2 \pm 1.46\text{‰}$ at the water–ice interface in the MY ice. Salinity of FY ice increased with increasing ice thickness, from $0.41 \pm 0.19\text{‰}$ in October to $3.39 \pm 1.75\text{‰}$ in March. We found very low concentrations of both Si and P in MY and FY ice in late fall ($<0.01 \mu\text{M}$), after the summer season of 1997. Mean integrated concentration of nutrients increased with the freeze-up of ice, reaching maximum values in the summer of 1998. Ice algal biomass was dominated by diatoms in the MY and FY ice, with more pennate than centric species. Species of dinoflagellates and green algae were subdominant. Green algae, typically confined to the upper part of the ice, were distributed throughout the ice thickness. During summer, the brackish-water green alga *Ulothrix implexa* formed long rope-like tufts attached to the hull of the icebreaker; development of this species has not previously been observed in the central Arctic Ocean. Biomass, cell abundance and chl *a* concentrations were high in the bottom sections of both MY and FY ice during the pre-freezing period, then decreased in winter and reached maximum values in spring and summer. The total algal biomass showed a pattern similar to chl *a* dynamics, decreasing from $1.7 \mu\text{g C l}^{-1}$ in October to values $<0.1 \mu\text{g C l}^{-1}$ in winter. Algal carbon biomass and chl *a* concentration co-varied significantly in the FY ice ($r^2 = 0.79$), but less so in the MY ice ($r^2 = 0.49$). An unexpected feature with respect to sea ice invertebrates was the absolute absence of living interstitial fauna within the interior of MY and FY sea ice. In addition, the under-ice fauna was species-poor. Comparisons of SHEBA results with historical data showed that the physical–chemical characteristics of sea ice and the biological structure of ice communities found in this study were very different from conditions during the 1970s. It is likely that the changes resulted from increased melting of the arctic ice pack over the last two decades.

© 2002 Published by Elsevier Science Ltd.

Keywords: Arctic Ocean; Canada Basin; Sea ice; Salinity; Nutrients; Algae; Invertebrate fauna

*Corresponding author. Tel.: +7-95-939-3872; fax: +7-95-939-1148.

E-mail addresses: migor@online.ru (I.A. Melnikov), hewelch@escape.ca (H.E. Welch), zhitina@hydro.biol.msu.ru (L.S. Zhitina).

1. Introduction

The Arctic Ocean is a major component of the world's atmosphere–ocean system; within this region, sea ice is a key environmental feature. The several meter thick sea ice cover affects the magnitude of both heat and matter fluxes from the atmosphere and upper ocean and supports unique and tightly coupled biological communities (Gran, 1904; Usachev, 1949; Horner, 1976; Melnikov, 1989). Observations carried out in the early 1970s demonstrated that time-scale characteristics, physical structure, and chemical compounds of sea ice, as well as species composition of biota in the sea ice cover, were stable within the vertical thickness of sea ice and over the geographical scale of the Arctic Ocean, despite interannual variability in environmental factors. These observations suggested that the sea ice cover was an integral and steady-state ecological system (Melnikov, 1997).

However, beginning in early 1990s, there has been a marked decrease of salinity within the upper mixed layer of the central Arctic Ocean, apparently due to melting of the sea ice as a consequence of warming in the Arctic (Carmack et al., 1995; McPhee et al., 1998; Morison et al., 1998). Oceanographic observations also showed that Atlantic water characteristics in the Canada and Makarov Basins in 1994 were at least 0.2°C warmer than indicated previously (Swift et al., 1997). As a physical layer between a warmer atmosphere and warmer upper ocean water, sea ice can be reduced in thickness by melting of both the upper and lower ice surfaces. Many oceanographic observations and general climate models predict a greenhouse-gas-induced warming in polar regions leading to a warming and freshening of the upper ocean and a substantial retreat of the sea ice cover (Alekseev et al., 1996; Carmack et al., 1995; Chapman and Walsh, 1993; Johannessen et al., 1995, 1999; Johnson et al., 1999; McPhee et al., 1998; Morison et al., 1998; Mysak and Venegas, 1998; Rothrock et al., 1999; Vinnikov et al., 1999). The most recent study using passive microwave data from satellites through 1996 has shown the Arctic sea ice extent decreasing by 2.9 ($\pm 0.2\%$) per decade (Cavalieri et al., 1997). Thus, an important question is: 'What changes are in the

modern Arctic Ocean and how do these environmental changes influence the biological and physical–chemical characteristics of the sea ice cover?'

In 1997–1998, in the Canada Basin of the Arctic Ocean, a USA/Canada project conducted a year-round ice-camp experiment, Surface HEat Budget of the Arctic Ocean/Joint Ocean Ice Study (SHEBA/JOIS), with the Canadian Coast Guard icebreaker *Des Groseilliers* as a central platform (Perovich et al., 1999). The primary goals of SHEBA were focused on issues of climate and heat budgets, and of JOIS on biological/chemical aspects within the sea ice–upper ocean system. The purpose of our component of the JOIS program was to examine nutrient and chlorophyll *a* (chl *a*) content, as well as species composition and seasonal dynamics of the biological communities associated with the sea ice and water–ice environment and then to use historical data we and others have obtained in the same region for understanding recent changes in the Arctic marine environment.

In this paper, sea ice terminology and nomenclature used are as discussed in Zubov (1945), Usachev (1949), Horner et al. (1988, 1992), and Melnikov (1997). Sea ice habitats are designated by their position within the snow (melt water)–ice surface, the sea ice interior and the water–ice interface. Within the sea ice interior we consider three sections: upper, middle and bottom, i.e., the upper sea-ice section bordered by the snow–ice surface, the bottom section bordered by the water–ice interface, and the middle section considered as a transitional section between the upper and bottom sections.

2. Materials and methods

This research was based on samples obtained during the SHEBA ice camp drift (SHEBA) from October 1997 (75°N and 142°W) to October 1998 (80°N and 166°W). From October 1997 to February 1998, SHEBA drifted westward over the Canada Abyssal Plain along 75°N, water depth ~3800 m. During February–September 1998, the ice camp crossed the Chukchi Plateau at water

depths of 300–1000 m in a northwest direction, and then again drifted northward to the Canada Abyssal Plain at 3300 m depth in September–October 1998 (Fig. 1). Observations were focused on collection of sea-ice cores, and water and plankton samples from the water–ice interface and under-ice water column. During the summer melt season, observations were also conducted in the melt ponds.

2.1. Sea ice observations

Multi-year (MY) and first-year (FY) ice cores were collected with a 12 cm AARI-type ice auger and/or a 10 cm fiberglass-barrel CRREL-type corer. Coring was conducted at two sites at a distance of 0.5 km (MY site) and 3 km (FY site) from the home ice floe. One or two ice core(s) were

collected per month at each site (Table 1). In addition to sampling at two sites, during March 3–4, and September 20–23, both MY and FY ice cores were collected in areas oriented in N, E, S, and W directions and at a distance of 5 km from the home ice floe. Cores were sectioned into 10 or 20 cm segments and transferred into 1- or 2-l plastic containers, and then melted *in vitro*. In this research we do not melt the ice cores in filtered seawater (Garrison and Buck, 1986) but used the same melting procedure that we have used in previous expeditions at the North Pole (NP) drifting stations, 1975–1981 (Melnikov, 1979): melting of sea-ice core subsamples in plastic containers at room temperature (20–22°C) during 4–5 h, in order to get the proper and representative results for a comparison of data sets obtained at the NP and SHEBA ice camps. Samples of ice

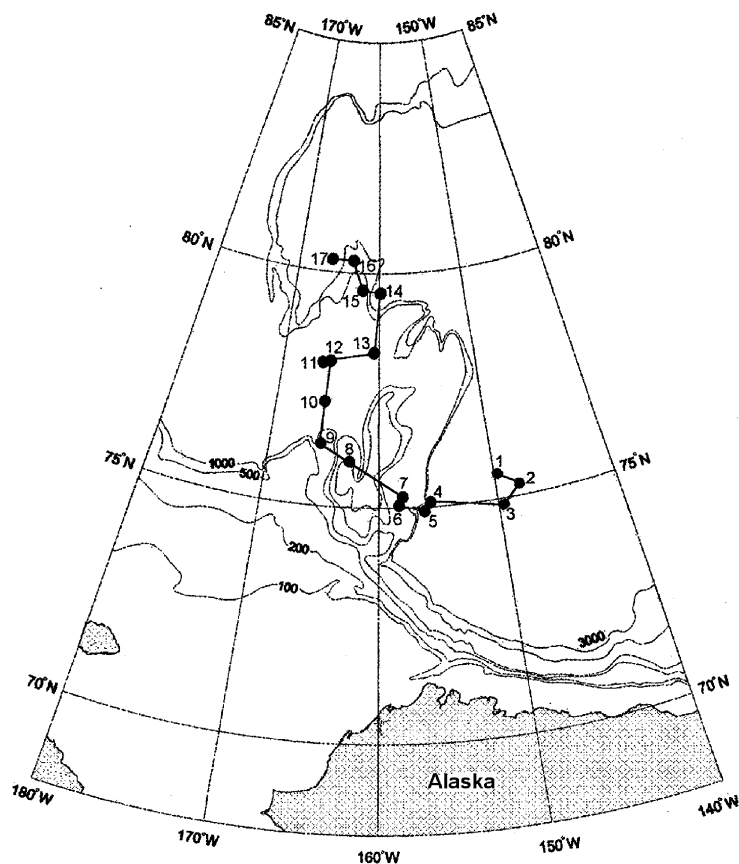


Fig. 1. SHEBA ice camp track in the Canada Basin of the Arctic Ocean, October 1997–October 1998.

Table 1
Multi-year and first-year sea-ice cores collected at the SHEBA ice camp

Ice core number	Ice core thickness (cm)	Date of sampling	Latitude (°N)	Longitude (°W)
<i>Multi-year ice</i>				
1	244 (10)	27 Oct. 97	75 17	143 31
2	235 (12)	12 Nov. 97	76 09	146 26
3	185 (9)	28 Nov. 97	75 07	147 33
4	216 (11)	10 Dec. 97	75 44	150 25
5	178 (9)	29 Dec. 97	75 17	149 59
6	177 (9)	12 Jan. 98	74 51	150 25
7	260 (13)	27 Jan. 98	74 51	155 38
8	281 (14)	18 Feb. 98	74 54	157 50
9	287 (5)	27 Feb. 98	75 05	159 47
10	394 (20)	27 Feb. 98	75 05	159 47
11	257 (13)	04 Mar. 98	75 08	159 40
12	194 (10)	04 Mar. 98	75 08	159 40
13	417 (22)	09 Mar. 98	75 28	160 18
14	287 (15)	29 Apr. 98	75 57	166 13
15	291 (15)	25 May 98	76 24	167 11
16	276 (16)	11 June 98	78 06	166 05
17	202 (12)	27 July 98	77 47	167 59
18	137 (9)	25 Aug. 98	78 24	158 15
19	382 (20)	13 Sep. 98	79 34	161 40
20	176 (8)	20 Sep. 98	80 11	164 41
21	147 (8)	20 Sep. 98	80 11	164 41
22	302 (15)	21 Sep. 98	80 14	164 42
23	223 (11)	22 Sep. 98	80 15	164 54
24	251 (13)	23 Sep. 98	80 21	165 32
<i>First-year ice</i>				
1	62 (6)	19 Oct. 97	75 20	144 29
2	66 (6)	27 Oct. 97	75 17	143 31
3	77 (7)	11 Nov. 97	76 09	146 23
4	79 (8)	26 Nov. 97	76 13	147 43
5	116 (6)	12 Dec. 97	75 41	150 44
6	95 (9)	27 Dec. 97	77 17	149 57
7	137 (7)	11 Jan. 98	74 53	150 12
8	150 (8)	24 Jan. 98	74 38	153 25
9	132 (7)	16 Feb. 98	74 53	157 50
10	134 (6)	27 Feb. 98	75 05	159 47
11	151 (6)	27 Feb. 98	75 05	159 47
12	140 (7)	03 Mar. 98	75 08	159 40
13	152 (7)	03 Mar. 98	75 08	159 40
14	171 (8)	09 Mar. 98	75 28	160 18
15	142 (8)	29 Apr. 98	75 57	166 13
16	138 (7)	25 May 98	76 24	167 11

Note: Number of ice sections is indicated in parentheses.

melt-water were processed immediately after melting on board *Des Groseilliers*. Salinity of melted samples was obtained through electronic conduc-

tivity measurements with a Beckman SoluBridge salinometer (model RB-5-349A, precision estimated as $\pm 0.1\text{‰}$). Subsamples for silicate (SiO_3^{2-}) and phosphate (PO_4^{3-}) concentration were assayed using a standard Technicon Autoanalyzer method (Atlas et al., 1971). Subsamples for fluorometric chl *a* determination were filtered onto Whatman GF/F glass fiber filters. Concentrations of chl *a* were determined on a R010 Turner Designs fluorometer after a 24-h extraction at 5°C in 90% methanol (modification of Parsons et al., 1984). Subsamples from each ice section were preserved with formaldehyde buffered with sodium acetate (final formalin concentration of ca. 1%) for floral and faunal species identification and enumeration by inverted light microscopy (Utermöhl, 1931). Only the pigments containing algal cells were counted.

All of the sea ice faunal species in each sample were enumerated and identified in a plankton counting tray with a light microscope at $300\times$ under laboratory conditions. Organism body size was measured and biomass was calculated by the formula: $W = K \times L^3$, where W is wet weight in mg, L is length in mm, and K is a coefficient (Vinogradov and Shushkina, 1987). After faunal identifications, the same samples were processed for identification of sea ice flora. Samples for cell enumeration and species identification were settled in Zeiss-type settling chambers for at least 12 h before counting with a Zeiss inverted light microscope. Horizontal transects across the bottom of the chamber were counted at $450\times$ for small, abundant organisms. The number of transects was dependent on the relative number of cells present in the chamber, but usually 1/10 of the chamber bottom was counted. A single transect through the center of the chamber was counted at $300\times$ for large, rare organisms. Cells, usually 10 or more for each taxon, were measured and cell numbers were transformed into carbon biomass according to the formulas of Strathmann (1967).

2.2. Water–ice interface

Samples from the under-ice surface were collected by pumping seawater through the ice hole to a plastic bucket. Seawater collections were carried

out biweekly from October 1997 to March 1998 and then continued in fall (September–October 1998). Subsamples of seawater for the determination of silicate, phosphate, and chl *a* concentrations were processed on board by the same methods described above for the ice cores.

Fifteen liter of seawater for microscopic analysis were concentrated in a reverse-flow filtration chamber through a 0.9 μm pore-size Nuclepore filter to a final volume of 3 ml. Samples to be analyzed by light microscopy were preserved with formaldehyde buffered with sodium acetate (final formalin concentration of 1%). For microzooplankton samples, 20 l of seawater were concentrated in another reverse-flow filtration chamber through a 10- μm mesh-size nylon gauze to a volume of 30 ml. Samples for microzooplankton were preserved with formaldehyde buffered with sodium acetate (final formalin concentration of 5%). Both under-ice flora and fauna samples were processed separately by inverted light microscopy (Utermöhl, 1931). All procedures for species enumeration, identification and biomass measurements were the same as described above for the sea ice samples.

Under-ice fauna were initially collected by a SCUBA-diver under the perennial ice in October–November, and later by scraping plankton net for a distance of 10 m along a marked rope at the under-ice surface (November–March). In both cases, plankton net was used with mesh size of 53 μm and a 40 cm \times 20 cm-wide flat top at the rectangular frame opening. The volume filtered was roughly calculated by multiplying the mouth area by distance towed; under-ice current velocities were not taken into account. In the laboratory the samples were washed on 53- μm mesh-size nylon gauze. The organisms were immediately fixed with a final formalin concentration of 5%. Each individual was identified in a plankton counting tray with a light microscope at 300 \times . All organisms in each sample were counted. For each individual, body size was measured, and biomass was calculated according to the equation of Vinogradov and Shushkina (1987).

In order to assess the influence of the seasonal upward migration of zooplankton in the under-ice fauna samples, vertical plankton tows were taken

with a Juday net with a 37-cm wide flat top and 150- μm mesh-size filtering cone (Table 2). Plankton tows were carried out from 0 to 1000 m in the water column, but here we consider only the species composition of zooplankton sampled from the upper 30 m. Plankton samples were concentrated on 150- μm mesh-size nylon gauze and fixed with 5% formaldehyde. Zooplankton collections were processed by standard methods used in planktonology (Kisilev, 1969). Since zooplankton abundances were low, a complete count of individual organisms in samples was possible. Biomass was calculated according to the equation of Vinogradov and Shushkina (1987).

In this paper, we discuss also the data on nutrients and chl *a* concentrations in the 0–30 m water column obtained during the SHEBA drift (courtesy by P. Wheeler).

2.3. Melt ponds

In the summer, when ice melting was most intense and the upper ice surface was marked by boundaries of melt ponds, investigations were carried out in the ponds formed initially from the melting of snow, and then of the ice proper. Melt ponds were chosen on the surface of the MY ice. Water samples for determination of salinity and chl *a* concentration were collected with a 10-l plastic bucket in the middle of each pond at approximately 1-week intervals in July–August, and sampling continued into September–October (Table 3). In September, when the air temperature decreased and melt ponds froze, both water and ice cores in the ponds were collected for salinity, chl *a* concentrations and species identification. These samples were processed as discussed above.

3. Results

3.1. Environmental conditions

The ice field where the ice camp was established in October 1997 was a consolidated MY ice floe, 1.7–2.1 m thick (J. Bitters, pers. comm.), marked with many shelves, hummocks, caverns, and cracks. Averaged over the year (October

Table 2

Samples from the water–ice interface (under-ice flora and fauna) and the 0–30 m water column (net plankton)

Sample number	Date of sampling	Latitude (°N)	Longitude (°W)
<i>Under-ice flora</i>			
1	15 Oct. 97	75 18	144 20
2	27 Oct. 97	75 17	143 31
3	11 Nov. 97	76 09	146 23
4	25 Nov. 97	76 15	147 41
5	10 Dec. 97	75 44	150 25
6	22 Dec. 97	75 19	150 01
7	12 Jan. 98	74 51	150 25
8	27 Jan. 98	74 51	155 38
9	10 Feb. 98	74 58	157 45
10	06 Mar. 98	75 13	159 57
11	13 May 98	76 11	165 12
12	26 May 98	76 27	167 30
13	10 Sep. 98	79 38	162 01
15	21 Sep. 98	80 14	164 42
16	01 Oct. 98	80 15	166 01
<i>Under-ice fauna</i>			
1	14 Oct. 97	75 18	144 20
2	23 Nov. 97	76 13	147 38
3	10 Dec. 97	75 44	150 25
4	22 Dec. 97	75 19	150 01
5	03 Jan. 98	74 58	149 38
6	12 Jan. 98	74 51	150 25
7	27 Jan. 98	74 51	155 38
8	17 Feb. 98	74 53	157 50
9	06 Mar. 98	75 13	159 57
<i>Net plankton</i>			
1	19 Dec. 97	75 32	150 17
2	30 Dec. 97	75 15	149 59
3	12 Jan. 98	74 51	150 25
4	30 Jan. 98	75 05	156 21
5	11 Feb. 98	74 54	157 47
6	26 Feb. 98	75 03	159 39
7	06 Mar. 98	75 13	159 57
8	03 May 98	76 00	165 30
9	22 May 98	76 20	166 35
10	17 June 98	77 17	166 28
11	02 July 98	78 07	166 48
12	15 July 98	78 05	166 08
13	01 Aug. 98	78 19	161 25
14	27 Aug. 98	79 34	160 01
15	10 Sep. 98	79 38	162 00
16	21 Sep. 98	80 14	164 42
17	01 Oct. 98	80 14	166 00

1997–October 1998), the 2 m air temperature was 0.6°C less than the climatological 2 m air temperature derived from data from 1979 to 1996

(Perovich et al., 1999). The melt season was long, lasting nearly 80 days. In comparison, melt seasons observed at ice stations of the former Soviet Union from 1960 to 1990 averaged 55 days and ranged from 20 to 83 days (Lindsay, 1998).

The under-ice water column was characterized by nearly isothermal conditions in the upper 30-m mixed layer and a strong pycnocline at 30–32 m (McPhee et al., 1998). In general, the mixed layer was close to the freezing point from fall through winter and into late spring. With the onset of the summer melt season (early June), the combination of a decrease in ice albedo and an increase in the area of open water and ponded ice allowed significant amounts of sunlight to be absorbed in the upper ocean, warming it. The warming continued through the summer, and the mixed layer reached a peak temperature of 0.3°C in late July. The summer warming of the mixed layer was more vigorous around leads. During June–July melt-water runoff from the upper surface of the ice formed a noticeable layer of fresh water beneath the ice. This layer was 1.3 m thick with a temperature near 2°C and salinity near 2‰ (Perovich et al., 1999). The melt season continued into late August with respect to surface melting and early October with respect to bottom melting of ice.

3.2. Physical and chemical environment

In the pre-freezing period of October–November 1997, the MY ice site consisted of undeformed ice with an average thickness of 221 ± 32 cm and an initial snow depth of 15–17 cm. The freeboard porous layer was 2–8 cm thick, milky white in color, and with a sharp upper boundary and an irregular lower boundary. The congelation ice structure was clearly differentiated from the snow–ice interface to the ice–water interface by several granular and porous layers 6–10 cm thick, which appeared to result from the freezing of surface melt-water that penetrated from the top to the bottom of the ice during the melting season. As the season progressed into winter, the ice grew and reached its maximum thickness of 270 ± 76 cm in April–May (Fig. 2a). With the onset of summer melt (early June) the MY ice thickness decreased

Table 3

Observations in three melt ponds at the SHEBA ice camp

Sample number	Date of observation	Latitude (°N)	Longitude (°W)	Note
1	10 July 98	78 05	165 54	Ice-free
2	13 July 98	78 04	166 22	Ice-free
3	18 July 98	78 12	166 07	Ice-free
4	26 July 98	78 32	165 24	Ice-free
5	07 Aug. 98	78 26	158 57	Ice-free
6	17 Sep. 98	79 45	162 47	Ice-covered
7	30 Sep. 98	80 10	165 49	Ice-covered
8	01 Oct. 98	80 14	166 01	Seawater open

to 219 ± 95 cm. The total MY ice thickness balance for the SHEBA area showed that during the winter period the ice increased by 75 cm but subsequently lost 70 cm through surface ablation and 40 cm through bottom ablation during the summer. Combining the growth and ablation gives a net thinning of the sea ice cover of ~ 35 cm during the SHEBA year (Perovich et al., 1999).

An initial bulk salinity of $1.43 \pm 0.96\%$ for MY ice was measured in October. This value increased to $2.97 \pm 1.87\%$ during the freeze-up in January and reached maximum values in the winter period (Fig. 2b). In the spring, salinity decreased to $0.94 \pm 0.5\%$ in May. During the annual MY ice observations, mean integrated salinity value was $0.1 \pm 0.8\%$ within the snow (melt water)–ice boundary and $3.2 \pm 1.46\%$ within the ice–water interface.

The FY ice site was located in an undeformed ice floe formed after freezing of the open water of a lead in late September (J. Bitters, pers. comm.). Initial ice thickness, measured from two ice cores in October, was 64 ± 0.2 cm with a snow depth of 7 cm. The ice at this site grew constantly during the winter period to a maximum of 171 cm in March and then started to decrease in April–May (Fig. 2c). Bulk integrated salinity of the FY ice increased with ice thickness, from an initial value of $0.41 \pm 0.19\%$ in October to $3.39 \pm 1.75\%$ in March (Fig. 2d). Snow depth increased during fall through winter, reaching an average depth of 34 cm by spring (Perovich et al., 1999).

The seasonal dynamics of mean integrated concentrations of silicate and phosphate (Fig. 3) showed very low values in MY ice in the late fall after the summer season of 1997. Silicate concen-

tration, which was undetectable in October, increased with the freeze-up of the ice to attain $0.45 \pm 0.19 \mu\text{M}$ in May, and with a further increase of up to $0.84 \pm 0.62 \mu\text{M}$ in the late summer (Fig. 3a). However, phosphate showed a different seasonal pattern, increasing slightly from 0.03 ± 0.03 in October to $0.07 \pm 0.05 \mu\text{M}$ in February, then rapidly decreasing to $0.01 \pm 0.05 \mu\text{M}$ in March, and subsequently increasing to $0.18 \pm 0.1 \mu\text{M}$ in July (Fig. 3b). The mean integrated concentration of silicate in the FY ice increased slowly during the winter period from $0.01 \mu\text{M}$ in October to $0.67 \pm 0.28 \mu\text{M}$ in May (Fig. 3c), but phosphate showed a double-maximum pattern increasing from $0.07 \pm 0.2 \mu\text{M}$ in October to $0.55 \pm 0.40 \mu\text{M}$ in January and April (Fig. 3d).

Vertical distribution of salinity and silicate values over the thickness of both MY and FY sea-ice cores was non-uniform (Fig. 4). We estimated that in the pre-freezing period the mean integrated salinity values of the MY ice cores were $<0.1\%$ in the snow–ice boundary, but were $0.77 \pm 0.66\%$ in the upper 0–80 cm section of the 244 cm ice thickness, $1.91 \pm 0.93\%$ in the middle 80–160 cm and $1.82 \pm 1.05\%$ in the bottom 120–244 cm. The mean integrated salinity values for the freezing period were $0.44 \pm 0.38\%$ in the upper 0–90 cm section of the average 270 cm ice thickness, $2.2 \pm 0.76\%$ in the middle 90–180 cm and $3.2 \pm 1.46\%$ in the bottom 180–270 cm. In the post-melting season the salinity values were estimated as $0.3 \pm 0.58\%$ in the upper 0–70 cm section of the average 219 cm ice thickness, $1.9 \pm 0.74\%$ in the middle 70–140 cm and $2.6 \pm 0.94\%$ in the bottom 140–219 cm (Fig. 4a). During the freeze-up season

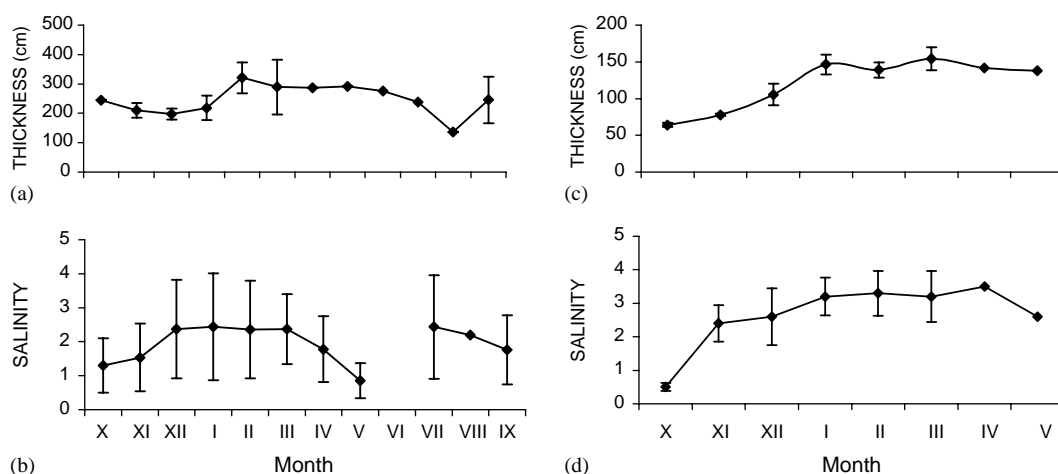


Fig. 2. Mean monthly thickness and integrated salinity in MY ice (a, b) during the period from October 1997 to September 1998 and FY ice (c, d) from October 1997 to May 1998. Salinity is integrated over the whole ice thickness. Monthly means and standard deviations are indicated for ice cores collected during the winter period. No data for the MY ice salinity in June 1997 due to sampling problems with beginning of the melt season. In July–September, the MY ice cores were collected at another site located at the distance of 500 m from the first one. Ice cores as in Table 1.

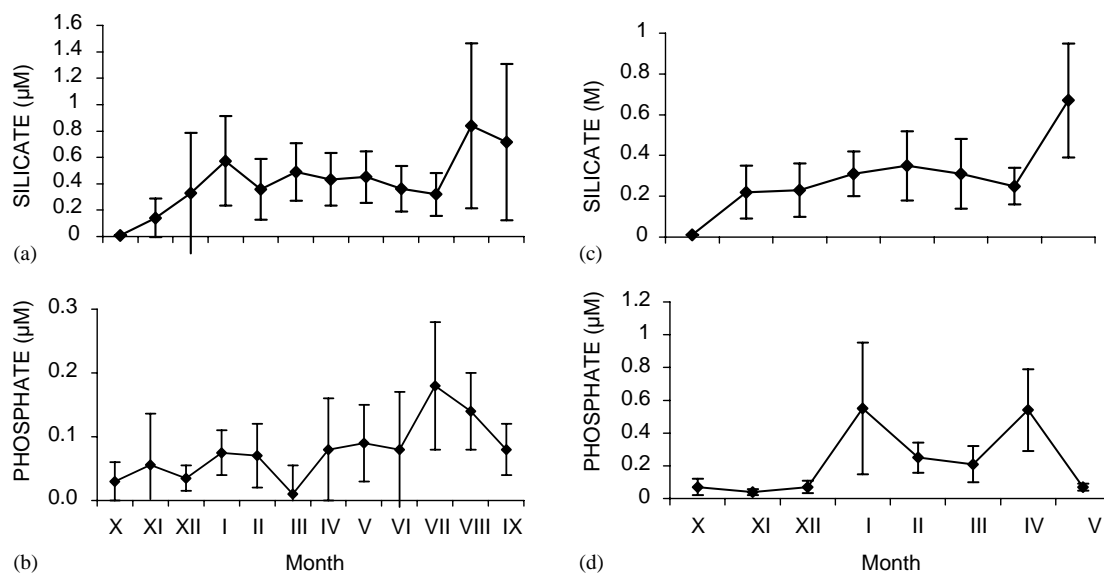


Fig. 3. Mean monthly integrated concentrations of silicate and phosphate in MY (a, b) during the period from October 1997 to September 1998 and FY ice (c, d) from October 1997 to May 1998. Mean concentrations are integrated over the whole sea-ice thickness. Ice cores as in Table 1.

nutrients (as silicate) decreased in the upper ice sections from values of 1.2–1.3 μM to values of 0.3–0.4 μM , but increased in the bottom sections to values of 0.9 μM (Fig. 4b).

Mean integrated salinity values in the FY ice increased consistently from the top to bottom sections with growth of sea-ice thickness (Fig. 4c). In the pre-freezing period, salinity values were

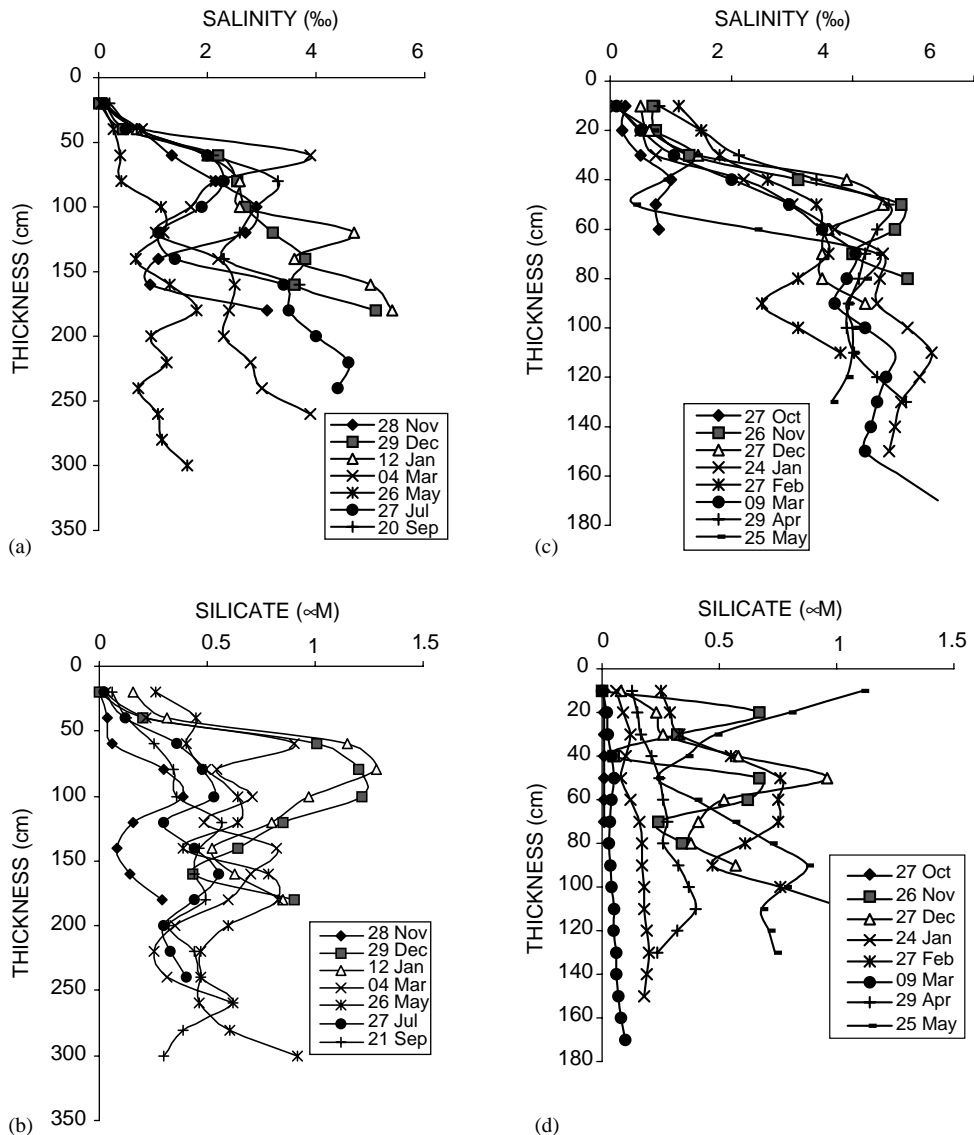


Fig. 4. Vertical profiles of salinity and silicate concentrations in MY (a, b) and FY (c, d) ice cores. Ice cores as in Table 1.

$0.2 \pm 0.04\text{‰}$ in the upper 0–20 cm section of the average 0.64 m thickness of ice, $0.56 \pm 0.21\text{‰}$ in the middle 20–40 cm, and $0.45 \pm 0.14\text{‰}$ in the bottom 40–64 cm. During the freezing period mean salinity values showed a steady increase to $1.32 \pm 1.16\text{‰}$ in the upper 0–60 cm section of the total 171 cm thickness of ice in March, $4.0 \pm 0.42\text{‰}$ in the middle 60–120 cm, and $4.6 \pm 0.44\text{‰}$ in the bottom 120–171 cm. Silicate concentrations were $<0.1 \mu\text{M}$ over the entire ice thickness in October, were

uniformly distributed in a range of $0.1\text{--}0.2 \mu\text{M}$ in January and March (Fig. 4d), and showed a double maximum in the May profile in the 0–20 cm upper section ($1.2 \mu\text{M}$) and in the 90–138 cm bottom section ($0.53\text{--}0.58 \mu\text{M}$).

3.3. Interstitial flora

A complete list of species associated with the sea ice interior (interstitial flora; Melnikov, 1997)

included 118 taxa belonging to the following groups: *Bacillariophyta*—80 species (68% of the total); *Dinophyta*—28 species (24%); *Chrysophyta*—4 species (3%); *Chlorophyta*—5 species (4%); and *Dictyochophyta*—1 species (1%) (Table 4). Of all identified diatoms, 25 species (31%) were in the centric group and 55 species (69%) in the pennate group. Species of the genera *Chaetoceros*, *Coscinodiscus*, and *Thalassiosira* dominated the centric diatoms, and species of *Fragilaria*, *Navicula*, and *Nitzschia* were dominant in the pennates. Among the non-diatom algae, dinoflagellates were a subdominant group with species in the genera *Dinophysis*, *Gymnodinium*, and *Protoperidinium*. Only 20 of the total 118 species were common in the samples of both the sea ice (MY and FY ice) and the ice–water interface. They were: the diatoms *Attheya septentrionalis*, *Chaetoceros convolutus*, *Ch. socialis*, *Leptocylindrus minimus*, *Cylindrotheca closterium*, *Melosira arctica*, *Nitzschia frigida*, *N. laevissima*, *N. longissima*, *N. neofrigida*, *N. promare*, *Nitzschia* sp., and *Thalassionema nitzschioides*; the dinoflagellates *Dinophysis arctica*, *Gymnodinium wulffii*, *Protoperidinium brevipe*, and *P. pallidum*; the chrysophyte *Groenlandiella brevispina*; the dictyochophyte *Dictyocha speculum* v. *octonarius*; and the green algae *Ancylonema nordenskioldii*. Similarity in the species composition between interstitial and cryopelagic flora was about 17%.

The total number of algal species found in samples of the MY ice was 84, in the FY ice, 33, and at the ice–water interface, 55. These included: *Bacillariophyta*—65, 27 and 30 species; *Dinophyta*—11, 3 and 21 species; *Chrysophyta*—4, 2 and 1 species; *Chlorophyta*—3, 1 and 2 species; and *Dictyochophyta*—1, 0 and 1 species, in MY ice, FY ice, and the ice–water interface, respectively. The prevalence of diatoms compared to other taxa of algae is a typical feature of the species composition of the sea ice interior flora. Pennate diatoms were more abundant than centric diatoms: 54 pennate and 11 centric diatom species in the MY ice and 20 and 7 in the FY ice. In all cases, species of the genera *Navicula* (16) and *Nitzschia* (10) were dominant among the pennate diatoms and constituted 36% of all diatom species. Species composition of the MY ice was more diverse

compared to that of FY ice: 84 and 33 species, respectively. All species observed in the samples of FY ice were also found in samples of the MY ice; differences between the two communities were caused mainly by the presence of rarer species such as the centric diatom *Odontella aurita* and the green alga *Scenedesmus quadricauda*.

3.4. Chlorophyll and biomass dynamics

The MY ice chl *a* values were lowest in winter, and showed a spring and summer maximum (Fig. 5). The mean chl *a* concentration integrated over the whole ice thickness was close to $0.2 \mu\text{g l}^{-1}$ during the winter period; highest observed values were $0.48 \mu\text{g l}^{-1}$ in March and $0.98 \mu\text{g l}^{-1}$ in July (Fig. 5a). The total algal biomass decreased from $4.4\text{--}5.3 \mu\text{g C l}^{-1}$ in October–December to $0.4 \mu\text{g C l}^{-1}$ in January, then slowly increased in spring (Fig. 5b). Unfortunately, there was a lack of data on algal biomass in summer, but the average integrated biomass value for the six sea-ice cores collected in September 1998 showed a mean value for algal biomass ($4.5 \pm 4.1 \mu\text{g C l}^{-1}$) similar to that found in the post-production season in October 1997 ($4.4 \pm 2.1 \mu\text{g C l}^{-1}$).

The bulk chl *a* concentration in the FY ice decreased rapidly with the onset of polar winter, from $0.33 \mu\text{g l}^{-1}$ in October to a minimum value of $0.05 \mu\text{g l}^{-1}$ in January, and then noticeably increased to values of $0.19\text{--}0.20 \mu\text{g l}^{-1}$ in spring (Fig. 5c). The total algal biomass showed a pattern similar to chl *a* dynamics, decreasing from $1.7 \mu\text{g C l}^{-1}$ in October to a value $<0.1 \mu\text{g C l}^{-1}$ in winter (Fig. 5d). Algal carbon biomass co-varied significantly with chl *a* concentrations in the FY ice ($r^2 = 0.79$), but these parameters were less well correlated in the MY ice ($r^2 = 0.49$) (Fig. 6).

The vertical distributions of chl *a* concentrations and of ice algal abundance and biomass were non-uniform over the thickness of both MY and FY sea-ice cores. Chl *a* concentrations showed a dramatic increase in summer in the bottom sections of the MY ice, reaching a maximum value of $9.23 \mu\text{g l}^{-1}$ by the end of July (Fig. 7a). These data suggest maximum sea ice algae activity in the bottom sections relative to ice algal activity in the

Table 4

Algae species present in samples collected in the multi-year (MY) ice, first-year (FY) ice and at the water–ice interface (under-ice)

Species	MY	FY	Under-ice
BACILLARIOPHYTA			
Centrophyceae			
<i>Actinocyclus curvatulus</i> Janisch	–	–	+
<i>Attheya septentrionalis</i> (Østrup) Crawford	+	+	+
<i>Aulacoseira</i> sp.	+	–	–
<i>Chaetoceros borealis</i> Bailey	–	–	+
<i>Ch. concavicornis</i> Mangin	+	–	+
<i>Ch. constrictus</i> Gran	–	–	+
<i>Ch. convolutus</i> Castracane	+	+	+
<i>Ch. diadema</i> (Ehrenberg) Gran	–	–	+
<i>Ch. fragilis</i> Meunier	–	+	–
<i>Ch. furcellatus</i> Baiely	+	–	–
<i>Ch. holsaticus</i> Schütt	–	+	–
<i>Ch. karianus</i> Grun	+	–	+
<i>Ch. radicans</i> Schütt	–	–	+
<i>Ch. socialis</i> Lauder	+	+	+
<i>Coscinodiscus asteromphalus</i> Ehrenberg	–	–	+
<i>Coscinodiscus concinnus</i> W. Smith	–	–	+
<i>Eucampia zodiacus</i> var. <i>recta</i> Ehrenberg	–	–	+
<i>Leptocylindrus minimus</i> Gran	+	+	+
<i>Melosira arctica</i> Dickie	+	–	+
<i>Odontella aurita</i> (Lymgbye) C.F. Agardh	–	+	–
<i>Proboscia alata</i> (Brightwell) Sundström	+	–	–
<i>Rhizosolenia setigera</i> Brightwell	–	–	+
<i>Thalassiosira gravida</i> Cleve	–	–	+
<i>Thalassiosira leptopus</i> (Grunow) Hasle & Fryxell.	+	–	–
<i>Thalassiosira nordenskiöldii</i> Cleve	–	–	+
Pennatophyceae			
<i>Amphora proteus</i> Gregory	+	–	–
<i>Cocconeis scutellum</i> Ehrenberg	+	–	–
<i>Cylindrotheca closterium</i> (Ehrenberg) Reimann & Lewin	+	+	+
<i>Diploneis didyma</i> (Ehrenberg) Ehrenberg	+	–	–
<i>D. litoralis</i> (Donkin) Cleve	+	+	–
<i>Diploneis</i> sp.	+	–	–
<i>Entomoneis gigantea</i> var. <i>septentrionalis</i> (Grunow) Poulin & Cardinal	+	–	–
<i>Entomoneis kjellmanii</i> (Cleve) Poulin & Cardinal	+	–	–
<i>E. paludosa</i> var. <i>hyperborea</i> (Grunow) Poulin & Cardinal	+	–	+
<i>Fragilaria islandica</i> Grunow	+	–	–
<i>F. striatula</i> Lyngbye	+	–	–
<i>Fragilariopsis cylindrus</i> (Grunow) Krieger	+	+	–
<i>F. oceanica</i> (Cleve) Hasle	+	–	+
<i>Gomphonema acuminatum</i> Ehrenberg	+	–	–
<i>Licmophora</i> sp.	+	–	+
<i>Manguinea</i> sp.	+	–	–
<i>Navicula directa</i> (W. Smith) Ralfs	+	–	–
<i>N. finmarchica</i> (Cleve & Grunow) Cleve	+	–	–
<i>N. gelida</i> Grunow	+	–	–
<i>N. glacialis</i> (Cleve) Grunow	+	–	–
<i>N. granii</i> (Jørgensen) Gran	+	+	–
<i>N. kariana</i> Grunow	+	–	–
<i>N. pelagica</i> Cleve	+	+	–
<i>N. punctulata</i> W. Smith	–	+	+

Table 4 (continued)

Species	MY	FY	Under-ice
<i>N. septentrionalis</i> (Grunow) Gran	+	—	—
<i>N. transitans</i> Cleve	+	+	—
<i>N. transitans</i> var. <i>derasa</i> (Grunow) Gran	+	—	—
<i>N. valida</i> Cleve & Grunov	+	—	—
<i>N. vanhoeffenii</i> Gran	+	+	—
<i>Navicula</i> sp.	+	+	—
<i>Navicula</i> sp.1	+	—	—
<i>Navicula</i> sp.2	+	—	—
<i>Nitzschia arctica</i> Cleve	+	—	—
<i>N. frigida</i> Grunow	+	+	+
<i>N. laevisissima</i> Grunow	+	+	+
<i>N. longissima</i> (Brebisson) Ralfs	+	+	+
<i>N. neofrigida</i> Medlin	+	+	+
<i>N. pellucida</i> Grunow	+	—	—
<i>N. polaris</i> Grunow	+	+	—
<i>N. promare</i> Medlin	+	+	+
<i>Nitzschia</i> spp.	+	—	—
<i>Nitzschia</i> sp.	+	+	+
<i>Pauliella taeniata</i> (Grunow) Round & Basson	+	—	—
<i>Phaeodactylum tricorutum</i> Bohlin	+	—	—
<i>Pinnularia quadratarea</i> (A. Schmidt) Cleve	+	+	—
<i>P. quadratarea</i> var. <i>bicontracta</i> (Østrup) Heiden	+	—	—
<i>P. quadratarea</i> var. <i>constricta</i> f. <i>interrupta</i> (Østrup) Heiden	+	—	—
<i>Pinnularia</i> sp.	+	—	—
<i>Pleurosigma elongatum</i> W. Smith	+	—	—
<i>Pleurosigma</i> sp.	+	—	—
<i>Pseudogomphonema arcticum</i> (Grunow) Medlin	+	—	—
<i>Pseudo-nitzschia delicatissima</i> (Cleve) Heiden	+	+	—
<i>Ps. seriata</i> (Cleve) Peregallo	+	+	—
<i>Synedropsis hyperborea</i> (Grunow) Hasley, Medlin & Syvertsen	+	—	—
<i>Thalassionema nitzschioides</i> (Grunow) Grunow ex Hustedt	+	+	+
DINOPHYTA			
<i>Amylax triacantha</i> (Jørgensen) Sournia	+	+	—
<i>Ceratium longipes</i> (Bailey) Gran	—	—	+
<i>Cochlodinium archimedes</i> (Pouch.) Lebour	—	—	+
<i>Dinophysis acuminata</i> Claparedes & Lachmann	—	—	+
<i>Dinophysis acuta</i> Ehrenberg	—	—	+
<i>Dinophysis arctica</i> Mereschk	+	+	+
<i>Dinophysis norvegica</i> Claparedes & Lachmann.	—	—	+
<i>Dinophysis rotundata</i> Claparedes & Lachmann	—	—	+
<i>Gymnodinium simplex</i> (Lohmann) Kofoed & Swezy	—	—	+
<i>Gymnodinium wulffii</i> Schiller	+	—	+
<i>Gymnodinium</i> sp.	+	—	—
<i>Gyrodinium</i> sp.	+	—	—
<i>Gonyaulax grindleyi</i> Reinecke	—	—	+
<i>Gonyaulax</i> sp.	+	—	—
<i>Protoperidinium bipes</i> (Paulsen) Balech	—	—	+
<i>P. breve</i> Paulsen	—	—	+
<i>P. brevipes</i> (Paulsen) Balech	+	—	+
<i>P. crassipes</i> (Kofoed) Balech	—	—	+
<i>P. curvipes</i> Ostenfold	—	—	+
<i>P. depressum</i> (Biale) Balech	—	—	+
<i>P. granii</i> (Ostenfold) Balech	—	—	+

Table 4 (continued)

Species	MY	FY	Under-ice
<i>P. pallidum</i> (Ostenfold) Balech	+	–	+
<i>P. pellucidum</i> Bergh	–	–	+
<i>P. pentagonum</i> (Gran) Balech	–	–	+
<i>P. quinquecorne</i> Abe	+	+	–
<i>P. thorianum</i> (Paulsen) Balech	+	–	–
<i>Protoperidinium</i> sp.	+	–	–
<i>Scrippsiella trochoide</i> (Stein) Loeblich III	–	–	+
CHRYSTOPHYTA			
<i>Groenlandiella brevispina</i> Kol	+	+	+
<i>Meringosphaera mediterranea</i> Lohmann	+	+	–
<i>M. tenerrima</i> Schiller	+	–	–
<i>Parapedinella reticulata</i> S.M. Pedersen & Thomson	+	–	–
DICTYOCOPHYTA			
<i>Dictyocha speculum</i> var. <i>octonarius</i> Ehrenberg	+	–	+
CHLOROPHYTA			
<i>Ancylonema nordenskioldii</i> Berggren	+	–	+
<i>Chlamydomonas nivalis</i> (Bau.) Wille	+	–	–
<i>Koliella</i> sp.	+	–	–
<i>Scenedesmus quadricauda</i> (Turpin) Brébisson	–	+	–
<i>Ulothrix implexa</i> (Kützinger) Kützinger	–	–	+
Total species	84	33	55

Note: “+” species was present; “–” species was not observed.

middle and upper sections, where mean chl *a* concentrations were $<1 \mu\text{g l}^{-1}$ during the summer season. The FY ice chl *a* values were highest in the top and middle ice sections in October–November (up to $1.45 \mu\text{g l}^{-1}$) and in the bottom sections in April–May ($0.52 \mu\text{g l}^{-1}$) (Fig. 7b).

Bacillariophyta dominated the algal biomass (as carbon) compared to other taxonomic groups in the MY ice, but *Chlorophyta* was subdominant (Fig. 8). Algal cell concentration and biomass were highest (maximum of 97 cells ml^{-1} and $19 \mu\text{g C l}^{-1}$) in the bottom section of the MY ice in the pre-freezing period, then decreased to about 5 cells ml^{-1} and $1 \mu\text{g C l}^{-1}$ in winter (Table 5). In September, after the summer season of 1998, we measured values of cell concentration and algal biomass in the upper, middle and bottom sections of the MY ice that were approximately similar to those found after the production season in October 1997. In the upper ice section, the most abundant species was the chrysophyte alga *Groen-*

landiella brevispina, reaching up to 20% of the total algal number and biomass. The diatom species *Nitzschia frigida*, *N. neofrigida*, *Cylindrotheca closterium* and *Fragilariopsis cylindrus* composed up to 90% of all cells in the bottom section of the MY ice. During the freezing period, *Groenlandiella brevispina* and *Navicula pelagica* dominated in the upper sections, and *Nitzschia frigida* and *N. neofrigida* in the bottom sections, of the MY ice.

Cell concentration and biomass values of algae in the FY ice were highest in October–November and were significantly less than values in the MY ice, decreasing to about 1 cell ml^{-1} and $0.1 \mu\text{g C l}^{-1}$ during the winter (Table 5). Two chrysophytes, *Groenlandiella brevispina* and *Meringosphaera mediterranea*, dominated within the upper and middle sections, and *Nitzschia frigida* and *N. neofrigida* dominated in the bottom sections, of the FY ice during the period of observations from October to March.

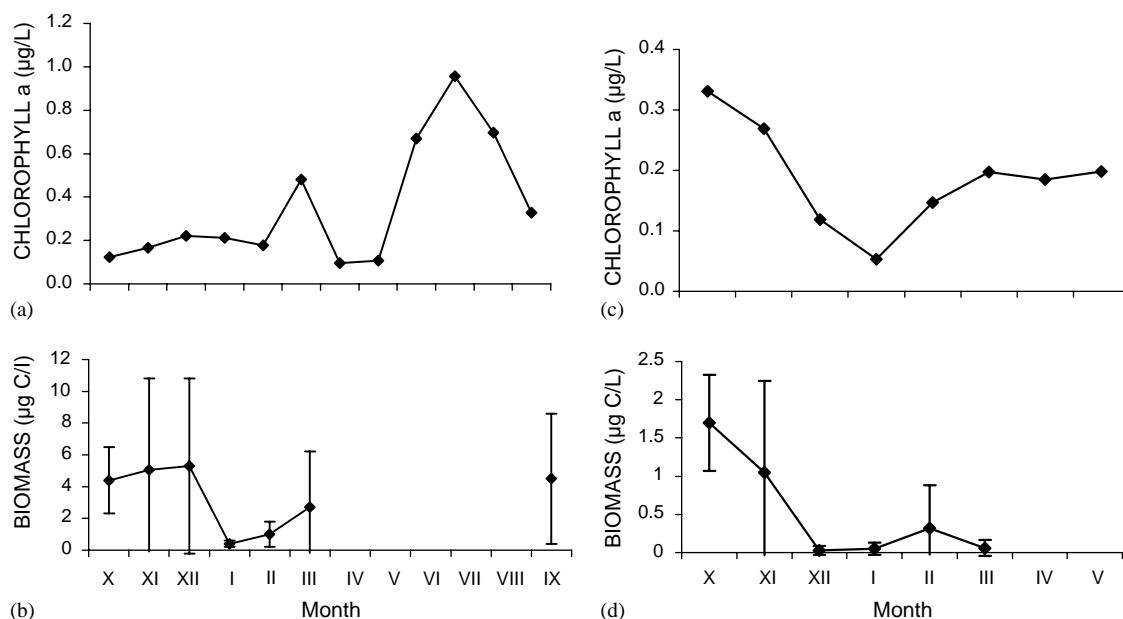


Fig. 5. Mean integrated chl *a* concentrations and total algal biomass as carbon in selected samples of the MY (a, b) and in the FY (c, d). No sea ice algae biomass data for the summer season.

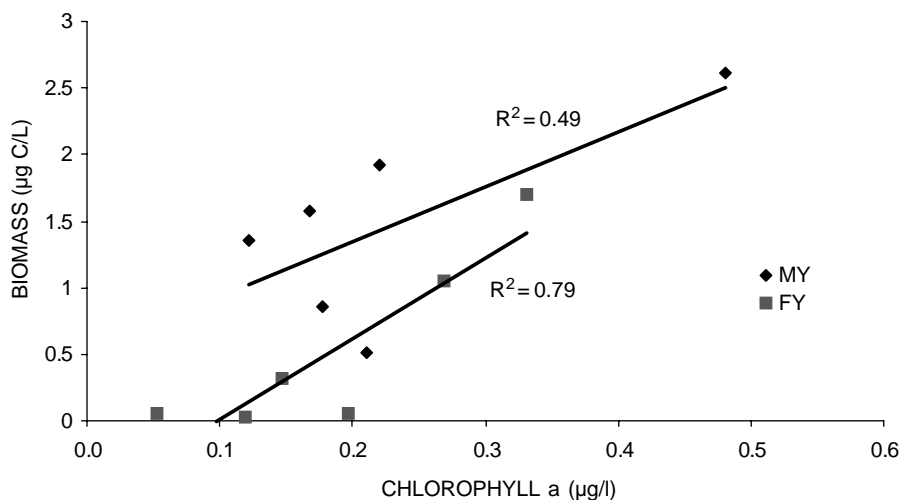


Fig. 6. Regression of sea ice algae biomass on chl *a* concentration. Algae biomass and chl *a* represent mean monthly integrated values over the ice thickness. Only winter ice cores (October 1997–March 1998) of both MY and FY are included in the regression analysis. The MY ice regression line is $y = 4.13x + 0.52$ and the FY ice is $y = 6.05 - 0.59x$. The correlation coefficient is significant for the FY ice ($r^2 = 0.79$, $p < 0.05$).

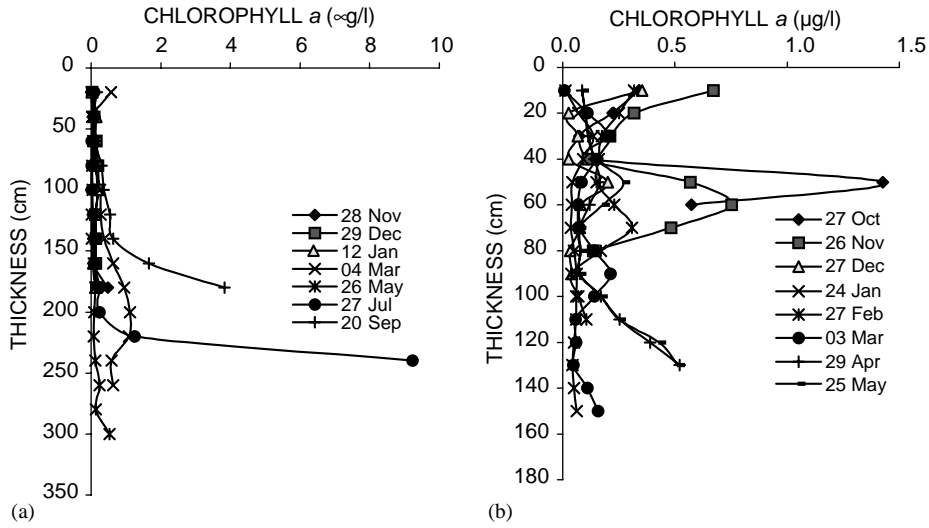


Fig. 7. Vertical profiles of chl *a* concentrations in selected samples from MY (a) and FY (b) ice cores. Ice cores as in Table 1.

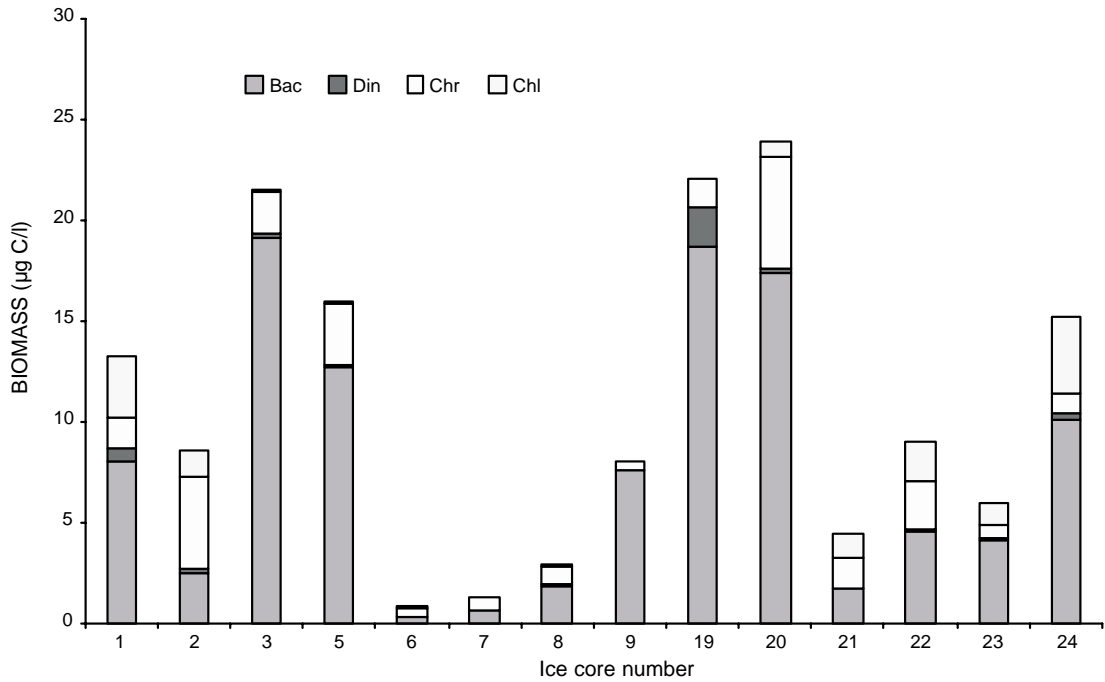


Fig. 8. Sea ice algae biomass of most abundant taxonomic groups: *Bacillariophyta* (Bac), *Dinophyta* (Din), *Chrysophyta* (Chr) and *Chlorophyta* (Chl) in the selected MY sea-ice cores. Ice core numbers are as in Table 1.

Table 5

Abundance and biomass (as carbon) of sea-ice algae in the upper (Up), middle (Md) and bottom (Bt) sections in selected MY and FY sea-ice cores

Ice core number	Concentration (cells ml ⁻¹)			Biomass (µg C l ⁻¹)		
	Up	Md	Bt	Up	Md	Bt
<i>Multi-year ice</i>						
1	7.8	15.9	17.3	2.4	4.2	6.6
2	1.8	18.1	27.9	0.8	3.4	4.5
3	2.1	8.5	97.1	0.5	1.8	19.3
5	15.6	64.9	8.7	2.7	11.6	1.6
6	1.4	3.2	0.5	0.2	0.4	0.2
7	1.4	1.7	3.8	0.2	0.3	0.8
8	4.7	3.3	8.8	0.6	0.4	2.0
9	18.9	20.4	1.5	6.8	1.0	0.4
19	5.0	18.1	92.6	0.8	2.3	19.0
20	9.6	47.1	66.3	2.0	9.3	12.8
21	8.3	7.9	8.6	1.4	1.1	2.0
22	10.9	6.2	34.0	2.0	1.1	5.9
23	4.1	9.3	13.5	1.0	1.0	4.0
24	0.0	21.3	54.1	0.0	7.0	8.3
<i>First-year ice</i>						
1	4	5.2	3.1	1.3	1.7	1.1
2	12	3.4	7.8	3.0	1.1	2.2
3	40.1	81.2	35.6	0.5	0.8	0.6
4	1.4	0	2.7	0.3	0.0	4.0
6	0	0.3	0	0.1	0.0	0.0
7	0	0.4	0	0.0	0.1	0.0
9	0	0	3.2	0.0	0.0	1.0
14	0	0.7	0	0.0	0.2	0.0

Note: Ice core numbers as in Table 1.

3.5. Under-ice flora

The under-ice flora included 55 species belonging to the following groups: *Bacillariophyta*—30 species (18 centric and 12 pennate); *Dinophyta*—21; *Chlorophyta*—2; *Chrysophyta* and *Dictyochophyta*—1 species each (Table 4). It is important to note that the abundance of non-diatom species was high: 25 (21%) of the total number of species. The under-ice flora (cryopelagic flora; Melnikov, 1997) was composed mainly of diatoms and dinoflagellates, with the genera *Chaetoceros*, *Coscinodiscus*, *Dinophysis*, and *Protoperidinium* dominating.

During the melting season of 1998 we observed the development of large-size diatom aggregations of plankto-benthic and benthic types, and brackish-water algal aggregations attached to the ice

substratum. The plankto-benthic aggregates of diatoms formed dense mucilaginous masses of various geometric configurations (spherical, elliptical, and formless) 10–15 cm in diameter and occurred fairly often between the ice floes (Fig. 9a). We observed these aggregations also between the ice floes and along the cracks and channels during the motion of the icebreaker *Des Groseilliers* on the way from the SHEBA site (81°N) to the ice edge (75°N) in October 1998. These free-floating masses were found under every type of sea ice, as they do not attach strongly to the ice surface and can be transported freely by water until the flow weakens although some aggregates remain in the holes at the ice surface. A quantitative assessment of aggregates could not be made because of technical problems. Two samples collected on September 9, 1998 were

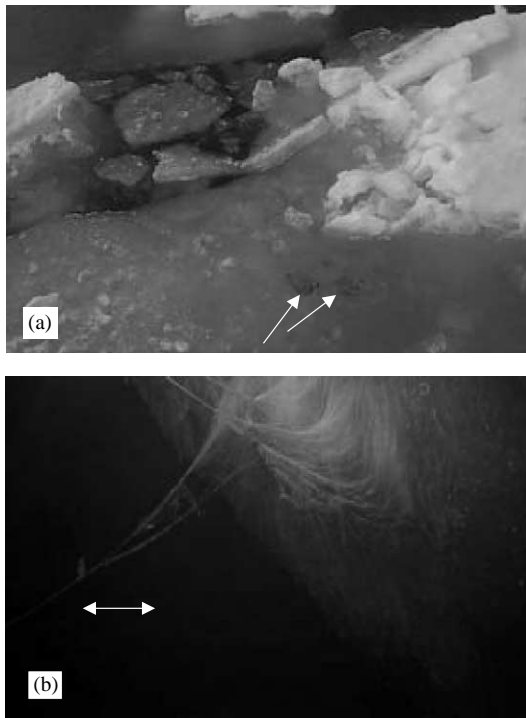


Fig. 9. Plankto-benthic type of diatom aggregates (dominant species *Chaetoceros socialis*, *Melosira arctica*, *Synedropsis hyperborea*) from the SHEBA ice camp, September 1998 (a). Arrows show clumps of diatoms on the ice surface. Green algal aggregations of *Ulothrix implexa* attached to the hull of the icebreaker *Des Groseilliers*, September–October 1998 (b). Scale is 1 m.

inspected for the systematic analysis of the algae that formed the aggregates. We found that the flora was composed mainly of diatoms, among which the dominant species were the centric species *Chaetoceros socialis* (43% of the total number) and *Melosira arctica* (23%) and the pennate species *Synedropsis hyperborea* (34%). Other algae included species of the genus *Nitzschia* (2%).

On October 5, three samples of diatom aggregations were collected from the bottom surface of the unreformed MY ice. Mats of algae 30–40 cm in length were strongly attached to the ice surface. In all samples, *Chaetoceros socialis* was the most abundant species (60% of the total species number), with subdominant species *Melosira arctica* (23%) and *Synedropsis hyperborea* (16%),

and *Nitzschia longissima* and others about 1%, respectively.

During the summer we observed the development of huge assemblages of the green alga *Ulothrix implexa* (Ulotrichales, Chlorophyceae). This alga started to grow in mid-July 1998 (C. Langis, pers. comm.). *U. implexa* formed 20–30 cm long rope-like tufts attached to the hull of the icebreaker *Des Groseilliers* from the water line to the bottom of the hull. During the sampling of 23 September 1998, strands of this alga were 3–5 m long (Fig. 9b). Surface water salinity values varied at that time over a range of 26–27‰. However, during the summer season the freshening of the under-ice environment was strongly influenced by sea ice melting and consequent flow of freshwater to the bottom of the ice cover (Eicken et al., in press). In this transitional zone between sea and fresh water, *U. implexa* (95% of the total cell number) formed multi-algal tufts in association with marine diatoms consisting of *Fragilariopsis oceanica* (3%), *F. cylindrus* (1%), *Nitzschia neofrigida* (0.4%), *Chaetoceros socialis* (0.35%), and *Synedropsis hyperborea* (0.15%).

3.6. Interstitial fauna

Fauna associated with the sea ice interior (interstitial fauna; Melnikov, 1997) was scarce in both the MY and FY ice cores (Table 6). Total taxa found included only 7 species: *Globigerina* sp., *Parafavella denticulata* and *Ptychocyclus obtusa* (Protozoa), *Jaschnovia brevis* and *Lucicutia polaris* (Copepoda), *Nematoda* sp. (Nematoda) and *Harpacticidae* sp. (Harpacticoida). All these species have been found previously in the interior of MY ice. In the FY ice samples only *Harpacticidae* sp. was found. The whole collection of interstitial fauna from the SHEBA ice camp consisted of non-living animals. We found single individuals of invertebrates and, as a rule, there were empty bodies of animals or their parts such as foraminiferan frustules, tintinnid loricas, nematode cuticles, and carapaces of copepods and crustacean nauplii. Distribution of animals within the ice thickness was irregular.

Table 6

Faunal species present in samples collected in the multi-year (MY) and first-year (FY) ice cores, at the water–ice interface (under-ice) and in the water column (0–30 m)

Species	MY	FY	Under-ice	0–30 (m)
PROTOZOA				
<i>Globigerina</i> sp.	+	–	+	+
<i>Radiolaria</i> gen. sp.	–	–	+	+
<i>Parafavella denticulata</i> Ehrenberg.	+	–	–	–
<i>Ptychocyclus obtusa</i> Brandt	+	–	–	–
HYDROZOA				
<i>Aglantha digitale</i> O.F. Müller	–	–	+	+
<i>Botrynema ellinorae</i> Hartlaub	–	–	+	–
<i>Aeginopsis laurentii</i> Brandt	–	–	–	+
SYPHONOPHORA				
<i>Dimophyes arctica</i> Chun	–	–	–	+
CTENOPHORA				
<i>Ctenophora</i> juv.	–	–	–	+
TURBELLARIA				
<i>Turbellaria</i> sp.	–	–	+	–
NEMATODA				
<i>Nematoda</i> sp.	+	–	+	–
POLYCHAETA				
<i>Thyphoscolex mulleri</i> Bush	–	–	–	+
<i>Pelagobia</i> sp.	–	–	–	+
<i>Polychaeta</i> larvae	–	–	–	+
OSTRACODA				
<i>Boroecia maxima</i> Brady and Norman	–	–	+	+
COPEPODA				
Calanoida				
<i>Calanus glacialis</i> Jaschnov	–	–	+	+
<i>Calanus hyperboreus</i> Krøyer	–	–	+	+
<i>Calanus marschallae</i> Frost	–	–	–	+
<i>Pseudocalanus minutus</i> Krøyer	–	–	+	+
<i>Microcalanus pygmaeus</i> Sars	–	–	+	+
<i>Spinocalanus longicornis</i> Sars	–	–	+	+
<i>Spinocalanus elongatus</i> Brodsky	–	–	+	–
<i>Ciridius obtusifrons</i> Sars	–	–	–	+
<i>Chiridiella abyssalis</i> Brodsky	–	–	+	–
<i>Jaschnovia brevis</i> Farran	+	–	+	–
<i>Pareuchaeta glacialis</i> Hansen	–	–	–	+
<i>Scolecithricella minor</i> Brady	–	–	–	+
<i>Scaphocalanus brevicornis</i> Sars	–	–	–	+
<i>Metridia longa</i> Lubbock	–	–	+	+
<i>Metridia pacifica</i> Brodsky	–	–	–	+
<i>Limnocalanus grimaldi</i> Guerne	–	–	+	–
<i>Acartia longiremis</i> Lilljeborg	–	–	+	–
<i>Lucicutia polaris</i> Brodsky	+	–	–	–

Table 6 (continued)

Species	MY	FY	Under-ice	0–30 (m)
CYCLOPOIDA				
<i>Oithona similis</i> Claus	—	—	+	+
<i>Oncaea borealis</i> Sars	—	—	+	+
<i>Oncaea notopus</i> Giesbrecht	—	—	+	—
<i>Lubbockia glacialis</i> Sars	—	—	+	—
<i>Mormonilla polaris</i> Sars	—	—	+	+
HARPACTICOIDA				
<i>Microsetella norvegica</i> Boeck	—	—	+	+
<i>Tisbe furcata</i> Baird	—	—	+	+
<i>Harpacticus superflexus</i> Willey	—	—	—	+
<i>Harpacticidae</i> sp.	+	+	—	+
CIRRIPEDIA				
<i>Cirripedia cypris</i>	—	—	+	—
MYSIDACEA				
<i>Mysis polaris</i> Holmquist	—	—	+	—
AMPHIPODA				
Hyperidea				
<i>Themisto abyssorum</i> Boeck	—	—	—	+
Gammaridea				
<i>Gammarus wilkitzkii</i> Birula	—	—	+	—
<i>Apherusa glacialis</i> Hansen	—	—	+	—
<i>Metopa longirama</i> Sars	—	—	+	—
<i>Pseudalibrotus nanseni</i> Sars	—	—	+	—
EUPHAUSIACEA				
<i>Thysanoessa raschii</i> Sars	—	—	—	+
PTEROPODA				
<i>Limacina helicina</i> Phipps	—	—	+	+
<i>Clione limacina</i> Phipps	—	—	—	+
CHAETOGNATHA				
<i>Eukrohnia hamata</i> Mobius	—	—	—	+
<i>Parasagitta elegans</i> Verril	—	—	+	+
APPENDICULARIA				
<i>Oikopleura vanhoffeni</i> Lohmann	—	—	+	+
<i>Oikopleura labradoriensis</i> Lohmann	—	—	+	+
<i>Fritillaria borealis</i> Lohmann	—	—	+	+
Total species	7	1	37	39

Note: “+” species was present; “—” species was not observed.

3.7. Under-ice fauna

The total list of species identified in samples from the water–ice interface and upper 35 m of the

water column included 59 species belonging to the following taxonomic groups (number of species in parentheses): *Copepoda* (18), *Amphipoda* (5), *Cyclopoida* (5), *Harpacticoida* (4), *Protozoa* (4),

Table 7

Average values of depth, salinity, and chlorophyll *a* concentrations observed at three melt ponds, SHEBA ice camp, summer 1998

Date	Melt water depth (cm)	Salinity (‰)	Temperature (°C)	Chl <i>a</i> ($\mu\text{g l}^{-1}$)	Note
10.07	20			0.046	Ice-free
13.07			0.2	ND	Ice-free
18.07				0.067	Ice-free
26.07				0.074	Ice-free
07.08		1.2		0.073	Ice-free
17.09					Ice-covered
30.09					Ice-covered
01.10					Seawater open

Hydrozoa (3), *Polychaeta* (3), *Appendicularia* (3), *Pteropoda* (3), *Chaetognatha* (2), *Syphonophora* (1), *Ctenophora* (1), *Turbellaria* (1), *Nematoda* (1), *Ostracoda* (1), *Cirripedia* (1), *Mysidacea* (1), *Euphausiacea* (1) (Table 6). Crustacea was the most abundant group (36 species) with dominance of calanoid copepods (27 species, 46% of the total).

Among the 59 species identified in both collections, 39 species were found in the 0–30 m depth zone and 37 species in the water–ice interface. Nineteen species of calanoid copepods were identified in the 0–35 m zooplankton catches and 18 species at the water–ice interface; however, only 11 species were common in both collections. These were: *Calanus glacialis*, *C. hyperboreus*, *Pseudocalanus minutus*, *Microcalanus pygmaeus*, *Spinocalanus longicornis*, *Metridia longa*, *Oithona similis*, *Oncaea borealis*, *Mormonilla polaris*, *Microsetella norvegica*, and *Tisbe furcata*. Four species of amphipods (*Gammarus wilkitzkii*, *Apherusa glacialis*, *Metopa longirama*, and *Pseudalibrotus nansenii*) and one mysid (*Mysis polaris*) were found near the water–ice interface.

Mean values of zooplankton abundance (Fig. 10) were approximately stable during the winter period and increased rapidly in May–June, reaching a maximum of $1232 \text{ individuals m}^{-3}$. Over the 4-week period between May 22 and June 17 (plankton stations 9 and 10), biomass increased approximately 20-fold, from 14 to 303 mg m^{-3} , but then subsequently decreased to 33 mg m^{-3} in September. The rapid increase in zooplankton abundance and biomass resulted from the seasonal vertical migration of dominant plankton species

such as *Calanus glacialis*, *C. hyperboreus*, *Microcalanus pygmaeus*, *Oithona similis*, and *Oncaea borealis* from the deeper Atlantic water, where they overwintered, to the surface water for the reproduction in summer. Appearance of these species in the 0–35 m water column was not coincident with the duration of their stay in the vicinity of the sea-ice surface. Decrease in both abundance and biomass in September–October suggests the onset of reverse migration of zooplankters to deeper waters. It is interesting that the copepod species *Calanus marshallae* and *Metridia pacifica* were found in the 0–35 m depth zone in February–May at stations 4–9, when the SHEBA ice camp drifted across the Chukchi Plateau with water depths of 300–1000 m (Melnikov and Kolosova, 2001). These species are typical for North Pacific waters but have not been noted in zooplankton collections during previous expeditions in the Beaufort Sea region of the Canada Basin (Grainger, 1965; Harding, 1966; Kosobokova, 1981; etc.).

3.8. Melt ponds

In the summer season many melt ponds, of irregular shapes and various depths, formed on the SHEBA ice camp floe (Fig. 11). Melt ponds covered more than 20% of the ice surface, with pond ice significantly thinned or partially melted through (Eicken et al., in press). Ponds were present from the last 10 days of June through late August. In response to seasonal cooling in September, surface melt-water in the ponds froze to an ice thickness of 10–15 cm. Three melt ponds

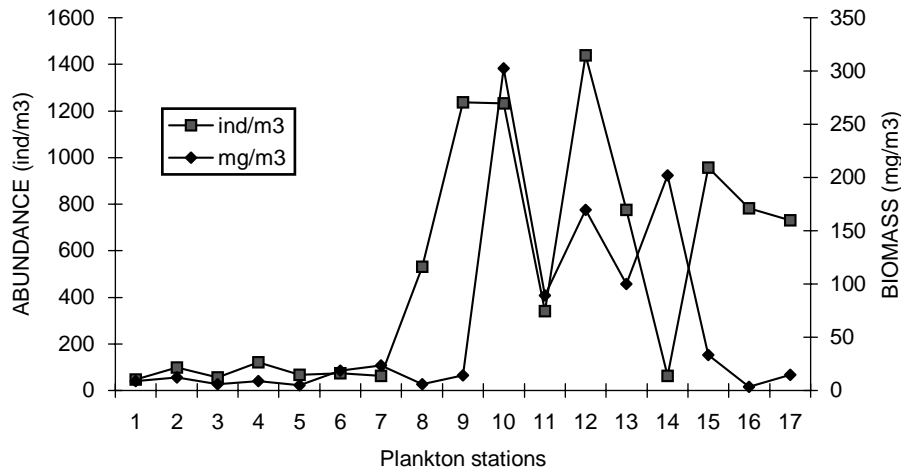


Fig. 10. Abundance and biomass of zooplankton in the upper 30 m of the water column. Plankton stations are as in Table 2.

were studied during the ice-free period in July–August, and during the ice-covered period in September–October (Tables 3 and 7).

In July, Pond #1 was $5 \times 14 \text{ m}^2$, oblong and regular, relatively deep (about 20 cm on average), with almost no drainage basin. Ponds #2 and #3 were large headwater ponds, irregular in shape, covering an area about $40 \times 40 \text{ m}^2$, with a drainage area twice as large (including the pond itself). They appeared to be “typical” ponds, and had drained and decreased in water depth (mean depth on the order of 10–15 cm) compared to Pond #1. Most of the snow had melted from the area by July, with the remainder present as large rounded “corn” snow grading into the eroded ice surface. During the July 10–August 7 sampling period, salinity and temperature in the melt-water ponds varied over the range 0.1–1.2‰ and 0.1–0.4°C, and chl *a* concentrations over the range 0.046–0.074 $\mu\text{g l}^{-1}$.

During the ice-covered period in fall, the depth of melt-water under newly formed ice ranged between 30 and 40 cm, and the average sea-ice thickness under the melt ponds ranged between 70 and 90 cm for all three ponds studied. The average integrated melt-water salinity values increased in Pond #1 to 4.8‰, in Pond #2 to 8.6‰, and in Pond #3 to 17.8‰. Temperatures of melt pond water also increased, averaging 0.5–0.8°C. The mean integrated chl *a* values in melt-water were in the range 0.011–0.016 $\mu\text{g l}^{-2}$.

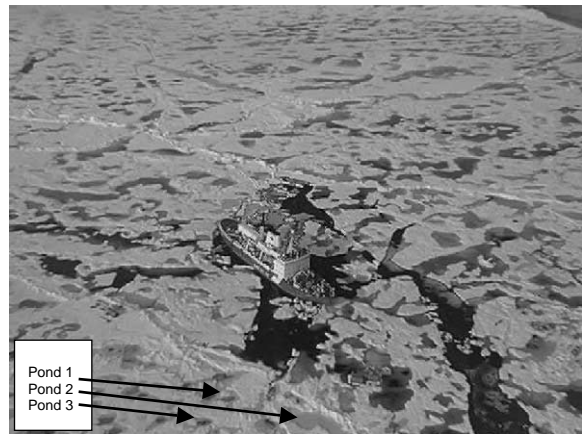


Fig. 11. Aerial photograph of the SHEBA field site with the CCG icebreaker *Des Groseilliers* and ice camp facilities, July 16, 1998. Melting ponds covered about 20% of the ice surface (Eicken et al., in press). Arrows indicate positions of ponds at the site.

Samples of melt-water from Pond #1 (September 30) and from Pond #3 (October 1) were collected for species identification of flora. These samples included both freshwater and typical marine species. A freshwater alga, *Chlamydomonas nivalis*, was dominant in both ponds sampled, representing 63% and 88% of total cell abundance, respectively. Subdominants were spores and the chrysophyte *Meringosphaera mediterranea* (36% and 9%, respectively). Several species of

marine diatoms (*Chaetoceros socialis*, *Cylindrotheca closterium*, *Fragilariopsis oceanica*, *Melosira arctica*, *Nitzschia frigida*, *Synedropsis hyperborea*, and *Thalassiosira* sp.) were found in both collections at abundances of about 1–3% of total cell number.

Invertebrate fauna in melt ponds was not found.

4. Discussion

Our observations of sea ice biological communities and nutrient dynamics can be compared to similar data sets collected in the period 1970–1980, during drifts of four prior expeditions: the former Soviet Union “North Pole-22” (NP-22) and “North Pole-23” (NP-23), and the USA T-3 and AIDJEX, ice camps. These ice camps covered the same general region of the Canada Basin as our study. Thus, we had an opportunity to assess changes in sea ice and under-ice parameters over a time scale of decades, which is pertinent to issues regarding global change in the Arctic Ocean. For data comparisons we used data sets obtained primarily at the NP-22 and NP-23 ice camps, which drifted in the region of the Beaufort Gyre during 1975–1981 (Belyaeva, 1980; Kosobokova, 1980; Melnikov and Kulikov, 1980; Melnikov et al., 1985; Melnikov and Bondarchuk, 1987; Melnikov, 1997), as well as other sources.

4.1. Sea ice

During the period 1967–1981, ice thickness ranged from 3–5 m (Buzuev, 1968; Koerner, 1973; Wadhams, 1983). In 1997–1998, sea ice was dramatically thinner, 1.4–2.1 m, in the region of the SHEBA drift in the Canada Basin. This remarkable change can be explained by a decrease of annualized cold day temperatures, which maintains the equilibrium thickness of ice. The sum of cold day temperatures (term of Zubov, 1945) decreased from 7000 (NP-22) in 1974–1975 to 6200 (SHEBA) in 1997–1998 for the same geographical region of the Arctic Ocean.

Mean integrated SHEBA values of the MY ice salinity were about 2-fold lower, and FY ice salinity values about 2-fold higher, compared to

ice salinities found during NP-22. A striking feature of the SHEBA ice samples was very low concentrations of Si in the MY and FY sea ice (0.40 and 0.28 μM , respectively) an order of magnitude lower than Si concentrations (3.7 μM in MY ice and 2.2 μM in FY ice) measured during NP-22. Decrease of Si values within the sea ice interior may be caused by an active release of these components during ice melt that, in turn, may limit sea ice diatom growth in the summer. The main features of chl *a* concentrations in the sea ice were lower values in the SHEBA MY ice samples, but higher values in the FY ice samples, compared to NP-22 data. The mean NP-22 chl *a* concentrations in MY sea ice (0.35 $\mu\text{g l}^{-1}$) were 2-fold higher than MY chl *a* concentrations found during SHEBA (0.16 $\mu\text{g l}^{-1}$). In contrast, SHEBA chl *a* stocks in the FY ice (0.18 $\mu\text{g l}^{-1}$) were 3-fold higher than were NP-22 FY ice chl *a* stocks (0.06 $\mu\text{g l}^{-1}$).

The list of identified algal species from NP-22 consisted of 171 taxa: 148 *Bacillariophyta*, 20 *Chlorophyta*, 1 *Dinophyta*, and 3 other species. The sea ice algal collection from the SHEBA consisted of only 88 taxa including 69 *Bacillariophyta*, 3 *Chlorophyta*, 11 *Dinophyta* and 5 other species. The prevalence of diatoms, and an obvious dominance of pennate compared to centric diatom species, were characteristic of both collections of sea ice flora. During NP-22, pennates were represented by 136 species (89% of all diatoms) and centrics by only 12 species (11%). During SHEBA, we found 55 species of pennate diatoms (80% of all diatoms) and 14 species of centrics (20%). Although the relative percentages of pennate and centric diatoms were similar in both floristic collections, the species abundance of pennate diatoms was 2-fold lower in the SHEBA collection compared to NP-22 data. The subdominance of *Dinophyta* in the SHEBA sea ice flora (11 species) compared with only one species of this group found during NP-22 was a major difference between the two data sets.

Decreasing numbers of pennate species and simultaneously increasing numbers of centric species and dinoflagellates in the SHEBA collection may be explained by the changing environmental factors observed recently within the sea ice substrate. We noticed in samples from the SHEBA

sea ice flora that diatoms had weakly silicified frustules, likely due to low concentrations of silicate in the ice. At the same time we also found that the chrysophytes *Groenlandiella brevispina* and *Meringosphaera mediterranea* were distributed within the ice interior from top to bottom in all sea ice samples from the SHEBA study. During NP 22, species of *Chlorophyta* and *Chrysophyta* were biotopically associated only with the upper sections of ice (Melnikov, 1997).

An intriguing feature of the MY and FY sea ice populations was a complete absence of living interstitial fauna within the sea ice interior in the SHEBA ice samples. Live interstitial fauna were detected in high numbers in the NP-22 sea ice samples. Ten species were described for the interstitial fauna from the NP-22 samples, including *Protozoa*, *Foraminifera*, *Acarina*, *Nematoda*, *Turbellaria*, *Harpacticoida* and *Amphipoda*. However, in both the MY and FY sea ice samples from the SHEBA data set, only fragments of foraminiferans, tintinnid ciliates, nematodes and copepods were found. The free-living nematode *Theristus melnikovi* was found by the thousands in the interior of MY ice samples during NP-22; but intact specimens of this nematode were never observed in any of the cores from the SHEBA MY and FY ice sites.

4.2. Water–ice interface

Recent melting of the arctic sea ice cover has resulted from the freshening and warming of the upper ocean during the past 20 years, as indicated by a comparison of temperature and salinity profiles for the upper 0–100 m of the Canada Basin obtained during the AIDJEX and SHEBA ice camps (McPhee et al., 1998). Over this period, salinity values have decreased by 3–4‰, and temperature have increased up to 0.4°C, within the upper 30 m of the water column. A sharp seasonal pycnocline formed between 30 and 32 m, and was stable through the SHEBA winter up to April. This was a significant barrier to turbulent mixing and capped the remnant mixed layer. It was clear that the freshening was widespread over the regions traversed by the SHEBA ice camp from October 1997 to April 1998.

The SHEBA mean values of Si concentrations in the 0–30 m water column were about 60% lower during the winter season, and about 40% lower in summer compared to the 1979–1980 NP-22 Si concentrations. In term of chl *a*, the average standing stock was 0.27 µg l⁻¹ during SHEBA and 0.16 µg l⁻¹ during NP-22. Higher chl *a* stocks may be explained by decreased ice thickness and thus more favorable light conditions for phytoplankton production at SHEBA as compared to conditions during NP-22.

At NP-22, the total number of algal species associated with the ice bottom surface was 21, with only one centric diatom (*Thalassiosira* sp.) and 20 typically benthic pennate diatoms. The SHEBA ice bottom collection included 30 diatoms: 18 pennate and 12 centric species. A marked increase in the number of centric diatom species (1 for NP-22 to 12 for SHEBA) was a major change in the under-ice flora. A second difference between these two data sets was a predominance of dinoflagellate species in samples from the water–ice interface at SHEBA (21 species), whereas only one dinoflagellate species was found during NP-22 (Belyaeva, 1980).

We also observed a significant difference in the ecology and taxonomy of algal mass accumulations beneath the ice. Beginning with the first Arctic Ocean expeditions, it has been well established that the centric diatom *Melosira arctica* forms large aggregations attached to the sea-ice surface (Gran, 1904; Usachev, 1949). In the Canada Basin of the Arctic Ocean (NP-23, summer 1977, 75–82°N, 138–179°E), Melnikov and Bondarchuk (1987) found massive accumulations of *Melosira arctica*, which formed huge mats and strands 4–6 m long on the bottom surface of MY ice. In all samples from the ice station NP-23 (1977), the diatom *Melosira arctica* was the most abundant species in benthic-type under-ice aggregations, making up 86–92% of the total cell number of diatoms. Similar observations of large mucilaginous masses of *Melosira arctica* were made in the eastern Arctic Ocean (Syvertsen, 1991) and in the central Arctic Ocean during the AOS in 1994 (Booth and Horner, 1997).

This type of aggregation was also observed at the SHEBA ice camp. On October 5, 1998, three

samples of diatom aggregations were collected from the bottom surface of the undeformed MY ice. Mats of algae 30–40 cm in length were strongly attached to the ice surface. In all samples, *Chaetoceros socialis* was the most abundant species (60% of the total number). *Melosira arctica* (23%) and *Synedropsis hyperborea* (16%) were subdominant species, with *Nitzschia longissima* and others about 1% of the total. Dominant and subdominant species in the plankto-benthic type of aggregates from NP-23 (77–78°N and 170–175°E, summer 1977) were also different compared to those found during SHEBA. During NP-23, these aggregates consisted almost completely of pennate diatoms: *Fragilaria striatula*, *Gomphonema kamtchaticum*, *Navicula vanhoef-fenii*, and *N. sigma* (Melnikov and Bondarchuk, 1987; Melnikov, 1997). It is interesting that the centric diatom *Melosira arctica* was not found in the plankto-benthic type of aggregates in the NP-23 collection but was present as a subdominant species in the collection from the SHEBA ice camp.

An interesting phenomenon at the SHEBA ice camp was the development of the green algae *Ulothrix implexa* (*Ulotrichales*, *Chlorophyceae*). It is well known that this species has a fairly wide ecological range, particularly in brackish habitats where environmental factors may show extreme daily or seasonal variations (Lokhorst, 1978). For example, *U. implexa* is frequently found in intertidal freshwater streams where the alga is exposed to seawater at high tide, as well as in estuaries and rivers, and at sites in the marine supralittoral exposed to an influx of fresh water. *U. implexa* can flourish on any solid substratum, e.g. wooden piles, and roots, stems and leaves of aquatic plants. In the Arctic, algae in the genus *Ulothrix* were initially described in non-tidal inland habitats such as the meso-oligohaline pools, lakes, and rivers of Franz-Josef Land (Shirshov, 1935). It was previously unknown that the brackish-water species *U. implexa* can also form extremely large-size aggregations in the high Arctic ice-covered marine environment.

Under-ice fauna from the SHEBA ice camp was relatively species-poor (Table 6). Within the water–ice interface, two general ecological groups can be distinguished: (1) autochthonous animals

permanently living on or near the underside of the ice; and (2) allochthonous animals temporarily present on the underside of the ice (Melnikov and Kulikov, 1980; Melnikov, 1989). According to this classification, within the SHEBA under-ice fauna we found:

1. An autochthonous ecological group including four amphipods (*Gammarus wilkitzkii*, *Apherusa glacialis*, *Metopa longirama*, *Pseudalibrotus nansenii*) and one mysid (*Mysis polaris*) with preferential occurrence of these animals of both sexes at all development stages on the bottom sea-ice surface.

2. An allochthonous group of animals including 11 typical zooplankton species (mainly calanoid copepods): *Calanus glacialis*, *C. hyperboreus*, *Pseudocalanus minutus*, *Microcalanus pygmaeus*, *Spinocalanus longicornis*, *Metridia longa*, *Oithona similis*, *Oncaea borealis*, *Mormonilla polaris*, *Microsetella norvegica*, and *Tisbe furcata*. The appearance of these species associated with the ice–water interface was caused by seasonal migration of these animals from the intermediate or Atlantic waters to surface habitats. Other planktonic organisms, such as protozoans, mollusks, ostracods, chaetognaths, and appendicularians, were found occasionally (several times per season) in the vicinity of the sea-ice surface (Table 6). Such occurrences were likely a result of vertical water mixing within the upper layer under the ice caused by strong current drift. For instance, after a strong storm on October 26, 1997, high turbulent mixing occurred in the 0–100 m water column (R. Pinkel, pers. comm.). Just after the storm, we observed many medusas and ctenophores attached to the ice surface, although we did not observe these animals during a dive on October 15 at the same location in calm weather before the storm.

In contrast to the species composition of the fauna associated with the water–ice interface during SHEBA, the autochthonous fauna observed during the NP-22 and NP-23 ice camps was more diversified. The NP-22 and NP-23 under-ice collections consisted of 12 species, including amphipods *Apherusa glacialis*, *Gammarus wilkitzkii*, *Gammaracanthus loricatus*, *Metopa* cf. *wiesei*, *Neupleustes* sp., and *Pseudalibrotus nansenii*, mysid *Mysis polaris*, copepods *Tisbe*

furcata and *Jaschnovia brevis*, the polychaete *Antinoella sarsi*, and fishes *Boreogadus saida* and *Arctogadus glacialis*, compared to only 7 autochthonous species found in this habitat during SHEBA. However, the NP-22 and NP-23 allochthonous group consisted of 9 species: *Calanus glacialis*, *Cyclopina schneideri*, *Harpacticus superflexus*, *Microcalanus pygmaeus*, *Microsetella norvegica*, *Oithona similis*, *Oncaea borealis*, *Pseudocalanus minutus*, and *P. elongatus*, two fewer than for SHEBA. The observed differences in species composition of the allochthonous group in these collections might be explained by differences in species structure of deep-water plankton, which are transient in the upper water column and the bottom surface of ice during seasonal migration of zooplankton. The decreased number of autochthonous species was probably a result of a fresher environment within the water–ice interface during SHEBA.

Thus, on the basis of comparisons between data collected at SHEBA and at NP-22 and NP-23, we conclude that: (i) during SHEBA, sea ice diatoms were rarer in terms of number of species and of cell abundance, for both MY and newly formed ice; (ii) freshwater chrysophytes previously found only on the upper-ice surface and/or within the upper sea ice layers (NP-22) were distributed within the entire sea-ice thickness (SHEBA); (iii) viable populations of invertebrate animals such as nematode, copepods, amphipods, and turbellarians previously found within the sea ice interior (NP-22) were not observed in the MY ice and newly formed sea ice (SHEBA); and (iv) for SHEBA samples, cryopelagic fauna associated with the bottom sea-ice surface as well as the under-ice zooplankton were also rarer in terms of species number and individual abundance compared to NP 22 and NP 23 observations.

The changes we found in composition and structure of the sea ice biological communities may be explained by the increased melting of the sea ice cover reported over the last decade (Cavalieri et al., 1997; Vinnikov et al., 1999; Maslanik et al., 1999; Rothrock et al., 1999; etc.). Environmental changes include: (i) intensive drainage of melt-water throughout the sea ice

interior (Eicken et al., in press); (ii) formation of a fresher water layer beneath the ice, 1.3 m thick with a temperature near 2°C and salinity near 2‰ (Perovich et al., 1999); and (iii) formation of a sharp pycnocline at a depth of 30–32 m (McPhee et al., 1998). Our documented changes in sea ice chemical and biological parameters suggest that in this region of the central Arctic, the water–ice system above the pycnocline has shifted toward a more brackish condition, compared to the more typical marine conditions found in previous studies.

Acknowledgements

We would like to thank the Canadian Coast Guard officers and crew of the icebreaker *Des Groseilliers* for their outstanding help during the SHEBA Ice Camp drift. Special thanks to captain Claude Langis for his interest and curiosity regarding *Ulothrix implexa* development under his icebreaker. We wish to thank also all participants of the SHEBA/JOIS project, who assisted both in field and in lab work. Special thanks are due to John (Jumper) Bitters, Bill Bosworth, Hajo Eicken, Bruce Elder, John Guvoni, Andy Heiberg, Dean Stewart and Terry Tucker for help in sea-ice core sampling, and Sandy Moore, Karen Thompson, Jim Watkins and Cathy Welch for lab data processing. We would also like to thank Barry Sherr and Pat Wheeler (Oregon State University, USA) for their kind offers to use their facilities. Evelyn and Barry Sherr are acknowledged for their assistance with the scientific editing of this paper. This work was supported by NSF grant OCE 9708088 to P. Wheeler, B. Sherr, and E. Sherr and by grants #99-05-64767 and #02-05-64357 of the Russian Foundation for Basic Research to I. Melnikov.

References

- Alekseev, G.V., Ivanov, V.V., Zakharov, V.F., Yanes, A.V., 1996. The Arctic Ocean in the global climate system. *Memoirs of the NIPR*, Special Issue 51, 267–276.

- Atlas, E.L., Hager, S.W., Gordon, L.I., Park, P.K., 1971. A practical manual for use of the Technicon Autoanalyzer in seawater nutrient analyses. Department of Oceanography, Oregon State University, Corvallis, OR. Revised OSU Technical Report, 215, Ref. No. 71-22, 48pp.
- Belyaeva, T.V., 1980. Phytoplankton of the NP-22 drift area. In: Vinogradov, M.E., Melnikov, I.A. (Eds.), *Biology of the Central Arctic Basin*. Nauka, Moscow, pp. 133–142.
- Booth, D.C., Horner, R.A., 1997. Microalgae on the Arctic Ocean Section, 1994; species abundance and biomass. *Deep-Sea Research II* 44, 1607–1622.
- Buzuev, A.Y., 1968. Certain statistical particularities in the multi-year ice thickness distribution. *Trudi AANII* 287, 76–84.
- Carmack, E.C., Macdonald, R.W., Perkin, R.G., McLaughlin, F.A., Pearson, R.J., 1995. Evidence for warming of Atlantic water in the southern Canadian Basin of the Arctic Ocean: results from the Larson-93 expedition. *Geophysical Research Letters* 22, 1061–1064.
- Cavaleri, D.J., Gloersen, P., Parkinson, C.L., Comiso, J.C., Zwally, H.J., 1997. Observed hemisphere asymmetry in global sea ice changes. *Science* 278, 1104–1106.
- Chapman, W.L., Walsh, J.E., 1993. Recent variations of sea ice and air temperatures in high latitudes. *Bulletin of the American Meteorological Society* 74 (1), 33–47.
- Eicken, H., Krouse, H.R., Kadko, D., Perovich, D.K. Tracer studies of pathways and rates of meltwater transport through Arctic summer sea ice. *Journal of Geophysical Research-Oceans*, in press.
- Garrison, D.L., Buck, K.R., 1986. Organism losses during ice melting: a serious bias in sea ice community studies. *Polar Biology* 6, 237–239.
- Grainger, H., 1965. Zooplankton from the Arctic Ocean and adjacent Canadian waters. I. Fisheries Research Board of Canada 22 (2), 543–564.
- Gran, H.H., 1904. Diatomacea from the ice-floes and plankton of the Arctic Ocean. *Scientific Research Norway North Polar Expedition* 4 (11), 3.
- Harding, G.C., 1966. Zooplankton distribution in the Arctic Ocean with the notes on life cycles. Master's Thesis, McGill University.
- Horner, R.A., 1976. Sea ice organisms. *Oceanography and Marine Biology Annual Review*, Aberdeen 14, 167–182.
- Horner, R., Syvertsen, E.E., Thomas, D.P., Lange, C., 1988. Proposed terminology and reporting units for sea ice algal assemblages. *Polar Biology* 12, 249–253.
- Horner, R.A., Ackley, S.F., Dieckmann, G.S., Gulliksen, B., Hoschia, T., Legendre, L., Melnikov, I.A., Reeburgh, W.S., Spindler, M., Sullivan, C.W., 1992. Ecology of sea ice biota 1. Habitat, terminology, and methodology. *Polar Biology* 12, 417–427.
- Johannessen, O.M., Miles, M., Bjorno, R., 1995. The Arctic's shrinking sea ice. *Nature* 376, 126–127.
- Johannessen, O.M., Shalina, E.V., Miles, M., 1999. Satellite evidence for an Arctic sea ice cover in transformation. *Science* 286, 1937–1939.
- Johnson, M.A., Proshutinsky, A.Y., Polyakov, I.V., 1999. Atmospheric patterns forcing two regimes of Arctic circulation: a return to anticyclone conditions? *Geophysical Research Letters* 26 (11), 1621–1624.
- Kisilev, I.A., 1969. Plankton of the seas and continental basin. Nauka, Leningrad, 657pp.
- Koerner, R.M., 1973. The mass balance of the sea ice of the Arctic Ocean. *Journal of Glaciology* 12, 123–129.
- Kosobokova, K.N., 1980. Seasonal variations in vertical distribution and age composition of populations of *Microcalanus pygmaeus*, *Oncaea borealis*, and *O. notopus* in the Central Arctic Basin. In: Vinogradov, M.E., Melnikov, I.A. (Eds.), *Biology of the Central Arctic Basin*. Nauka, Moscow, pp. 167–182.
- Kosobokova, K.N., 1981. Zooplankton of the Central Arctic Basin. Master's Thesis, Inst.Okeanol., Akad. Nauk USSR.
- Lindsay, R.W., 1998. Temporal variability of the energy balance of thick Arctic pack ice. *Journal of Climatology* 11, 313–331.
- Lokhorst, G.M., 1978. Taxonomic studies on the marine and brackish-water species on *Ulothrix* (*Ulotrichales*, *Chlorophyceae*) in Western Europe. *Blumea* 24, 191–299.
- Maslanik, J.A., Serreze, M.C., Agnew, T., 1999. On record reduction in 1998 Western Arctic sea ice cover. *Geophysical Research Letters* 26 (13), 1905–1908.
- McPhee, M.G., Stanton, T.P., Morison, J.H., Martinson, D.G., 1998. Freshening of the upper ocean in the Arctic: is perennial sea ice disappearing? *Geophysical Research Letters* 25, 1729–1732.
- Melnikov, I.A., 1979. Cryobiological observations in the Central Arctic Basin (methods and some results of studies). *Oceanology* 19 (1), 150–155.
- Melnikov, I.A., 1989. Ecology of Arctic Ocean cryopelagic fauna. In: Herman, Y. (Ed.), *The Arctic Seas: Climatology, Oceanography, Geology and Biology*. Van Nostrand Reinhold, New York, pp. 235–255.
- Melnikov, I.A., 1997. *The Arctic Sea Ice Ecosystem*. Gordon and Breach Sci. Publ., London, 204pp.
- Melnikov, I.A., Bondarchuk, L.L., 1987. To the ecology of the mass aggregations of colonial diatom algae under the Arctic drifting sea ice. *Oceanology* 27 (2), 317–321.
- Melnikov, I.A., Kolosova, E.G., 2001. The Canada Basin zooplankton in recent environmental changes in the Arctic Ocean. In: Semiletov, I.P. (Ed.), *Proceedings of the Arctic Regional Center*, Vol. 3. Pacific Institute of Oceanology, Vladivostok, pp. 165–176.
- Melnikov, I.A., Kulikov, A.S., 1980. Cryopelagic fauna of the Central Arctic Basin. In: Vinogradov, M.E., Melnikov, I.A. (Eds.), *Biology of the Central Arctic Basin*. Nauka, Moscow, pp. 97–111.
- Melnikov, I.A., Korzhikova, L.I., Nalbandov, Yu.R., 1985. Content and dynamic of nutrients and organic matter in snow-ice cover of the Arctic Basin. In: Bordovsky, O.K., Shirshov, P.P. (Eds.), *Hydrochemical Processes in the Ocean*. Institute of Oceanology, Acad. Sci. USSR, Moscow, pp. 86–89.

- Morison, J.H., Steele, M., Andersen, R., 1998. Hydrography of the upper Arctic Ocean measured from the nuclear submarine USS Pargo. *Deep-Sea Research I* 45, 15–38.
- Mysak, A.M., Venegas, S.A., 1998. Decadal climate oscillations in the Arctic: a new feedback loop for atmosphere–ice–ocean interactions. *Geophysical Research Letters* 25 (19), 3607–3610.
- Parsons, T.R., Maita, Y., Lalli, C.M., 1984. *A Manual of Chemical and Biological Methods for Seawater Analysis*. Pergamon Press, Toronto.
- Perovich, D.K., Andreas, E.L., Curry, J.A., Eiken, H., Fairrall, C.W., Grenfell, T.C., Guest, P.S., Intrieri, J., Kadko, D., Lindsay, R.W., McPhee, M.G., Morison, J., Moritz, R.E., Paulson, C.A., Pegau, W.S., Persson, P.O.G., Pinkel, R., Richter-Menge, J.A., Stanton, T., Stern, H.M., Tucker III, W.B., Uttal, T., 1999. Year on ice gives climate insights. *Eos* 80(41).
- Rothrock, D.A., Yu, Y., Maykut, G.A., 1999. Thinning of the Arctic sea-ice cover. *Geophysical Research Letters* 26 (23), 3469–3472.
- Shirshov, P.P., 1935. Eco-geographical description of the fresh water algae from Novaya Zemlya and Franz-Josef Land. *Trudy Institute of Arctic–Antarctic* 14, 73–162.
- Strathmann, R.R., 1967. Estimating the organic carbon content of phytoplankton from cell volume or plasma volume. *Limnology and Oceanography* 12, 411–418.
- Syvertsen, E.E., 1991. Ice algae in the Barents Sea: types of assemblages, origin, fate, and role in the ice-edge phytoplankton bloom. *Polar Research* 10, 277–287.
- Swift, J.H., Jones, E.P., Aagaard, K., Carmack, E.C., Hingston, M., Macdonald, R.W., MacLaughlin, F.A., Perkin, R.G., 1997. Waters of the Makarov and Canada Basin. *Deep-Sea Research II* 44, 1503–1529.
- Usachev, P.I., 1949. The microflora of polar ice. *Academia Nauk USSR, Trudy Institute of Oceanology* 3, 216–259.
- Utermöhl, H., 1931. Neue Wege in der quantitative Erfassung des Planktons. *Verhandlungen der Internationalen Vereinigung für theoretische und angewandte Limnologie* 5, 567–596.
- Vinnikov, K.Y., Robok, A., Stouffer, R., Walsh, J., Parkinson, C., Cavalieri, D., Mitchell, J., Garrett, D., Zakharov, V., 1999. Global warming and northern hemisphere sea ice extent. *Science* 286 (5446), 1934–1937.
- Vinogradov, M.E., Shushkina, E.A., 1987. *Function of the plankton communities in the epipelagic of oceans*. Nauka, Moscow, 240pp.
- Wadhams, P., 1983. Sea ice thickness distribution in Fram Strait. *Nature* 305, 108–111.
- Zubov, N.N., 1945. *Arctic Ice*. Izd. Glavsevmorputi, 360pp (US Navy Hydrographic Office, Translation 217, 1963; available as AD426972 from NTIS, Springfield, VA).